

# Nonlinear Functional Output Regression: a Dictionary Approach

Dimitri Bouche<sup>\*</sup>, Marianne Clausel<sup>\*\*</sup>, François Roueff<sup>\*</sup>, and Florence d'Alché-Buc<sup>\*</sup>

<sup>\*</sup>IDS, Télécom Paris, IP Paris

<sup>\*\*</sup>Institut Elie Cartan de Lorraine, University of Lorraine

## Abstract

Many applications in signal processing involve data that consists in a high number of simultaneous or sequential measurements of the same phenomenon. Such data is inherently high dimensional, however it contains strong within observation correlations and smoothness patterns which can be exploited in the learning process. A relevant modelling is provided by functional data analysis. We consider the setting of functional output regression. We introduce Projection Learning, a novel dictionary-based approach that combines a representation of the functional output on this dictionary with the minimization of a functional loss. This general method is instantiated with vector-valued kernels, allowing to impose some structure on the model. We prove general theoretical results on projection learning, with in particular a bound on the estimation error. From the practical point of view, experiments on several data sets show the efficiency of the method. Notably, we provide evidence that Projection Learning is competitive compared to other nonlinear output functional regression methods and shows an interesting ability to deal with sparsely observed functions with missing data.

## 1 Introduction

In a large number of fields such as biomedical signal processing, speech and acoustics and climate science, data consists of a high number of simultaneous or sequential measurements of different aspects of the same phenomenon. Such data is inherently high dimensional, however it contains strong within-observation correlations and smoothness patterns which can be utilized in the learning process. A possible way to do so is to represent those observations as functions rather than vectors, opening the door to Functional Data Analysis (FDA) [Ramsay & Silverman \(2005\)](#), a research area that has recently attracted a growing interest due to the ubiquity of embedded devices and sensor data. In practice, FDA relies on the assumption that the sampling rate at which data are collected is high enough to get functional observations. Of special interest is the general problem of functional-output regression in which the output variable to regress is a function and no specific assumption is made on the input variable that can be of any type, including functions.

While functional linear model have received a great deal of attention—see [Ramsay & Silverman \(2005\)](#), [Morris \(2015\)](#) and references therein—non-linear ones have been less studied. Extending this framework of additive function on function regression, [Reimherr & Sriperumbudur \(2017\)](#) proposes to replace the linear interaction between the regression function and the

input functions by a tri-variate function lying in a Reproducing Kernel Hilbert Space (RKHS) thus introducing a non-linear additive function on function regression model. In another nonparametric approach, [Ferraty & Vieu \(2006\)](#) introduces several variations of the Nadaraya-Watson kernel estimator devoted to functional-output regression. [Oliva et al. \(2015\)](#) rather tackles the problem of function-to-function regression by projecting both input and output functions on orthogonal bases and then perform separate Kernel Ridge Regressions (KRR) to predict the output coefficients from the input ones. Extending kernel methods to functional data, [Lian \(2007\)](#) introduces a function-on-function KRR. In that context, [Kadri et al. \(2016\)](#) explores the possibilities offered by the output operator and solves the functional KRR problem by approximately inverting an infinite dimensional linear operator.

In this paper we propose a novel machine learning approach to functional output regression. To learn to predict an output function, we fix a dictionary which span approximates the output space, and learn to predict the representation coefficients on this dictionary from the input. To do so, we minimize a functional loss measuring the discrepancies between the output observations and our output function expressed as a linear expansion on the dictionary. On the one hand, as in other works [Oliva et al. \(2015\)](#), we benefit from the important background in function approximation with dictionaries—see for instance [Meyer \(1993\)](#) and [Mallat \(2008\)](#). On the other hand, our work stands out because we predict the representation of the output function conditionally on the input. We call this general approach *Projection Learning*. Moreover, in practice, when only noisy sampled evaluations of the (training) output functions are observed, *Projection Learning* can still be applied using a functional loss directly estimated on the noisy sampled observations. As opposed to [Oliva et al. \(2015\)](#) which proceeds in two steps— firstly representing the data on a truncated orthogonal basis and secondly using the obtained coefficients as vector data—we proceed in a single step without performing a prior smoothing. Any machine learning algorithm outputting vectors can then be used for *Projection Learning*. However learning to predict an output function by predicting its decomposition on a dictionary raises an interesting issue of regularization. How to convey a penalty on the nature of predicted output functions ?

To answer to this question, the framework of vector-valued Reproducing Kernel Hilbert Space (vv-RKHS) [Micchelli & Pontil \(2005\)](#) is especially attractive. Vv-RKHSs extend the scope of kernel methods to vector-valued functions by means of Operator-Valued Kernels (OVK). Learning in vv-RKHS typically rely on Minimal Norm Interpolant Representer Theorem. Regularization can be tailored through the choice of the OVK which directly defines the vv-RKHS norm [Alvarez et al. \(2012\)](#). For the interested reader, we give a brief overview of OVKs and vv-RKHSs in the Section A of the Supplementary. Our contributions can be summarized as follows.

- We introduce *Projection Learning*, a novel framework to handle functional-output regression predicting decomposition coefficients of the output on a dictionary that we regress directly on the input data by minimizing a functional loss.
- We solve this new task relying on vv-RKHS. We call this instantiation *Kernel-based Projection Learning (KPL)*. This kernelized framework allows for regressing function on any input type of data. On the theoretical side, we prove a bound on the estimation error under some classical assumptions on the dictionary.
- Relaxing the assumption of observing each output function at a high and regular sampling rate, we define a practical variant of KPL where the functional loss is approximated on the observed samples of the training output functions.
- We show the efficiency of KPL on a toy dataset and two real datasets, and compare it with three non-linear function-to-function regression methods we re-implemented.

The paper is structured as follows. Section 2 introduces *Projection Learning* as a general approach. Section 3 presents how to solve it in the context of vv-RKHS taking advantage of OVKS. We propose as well an algorithm working directly with discretized functional data and support the method theoretically with a bound on its estimation error. In Section 4, we briefly present other existing methods for nonlinear functional-output regression. In Section 5 numerical experiments show the performance and efficiency of KPL compared to the methods presented in the previous section. Finally, Section 6 presents our conclusions and perspectives for future work.

**Notations**  $[N]$  denotes the set  $\llbracket 1, N \rrbracket$ .  $\mathcal{F}(\mathcal{X}, \mathcal{Y})$  stands for the set of functions  $\mathcal{X} \rightarrow \mathcal{Y}$ . If  $\mathcal{Y}_0, \mathcal{Y}_1$  are two Hilbert spaces,  $\mathcal{L}(\mathcal{Y}_0, \mathcal{Y}_1)$  denotes the set of bounded linear operators from  $\mathcal{Y}_0$  to  $\mathcal{Y}_1$ , and we use the shorter notation  $\mathcal{L}(\mathcal{Y}_0) := \mathcal{L}(\mathcal{Y}_0, \mathcal{Y}_0)$  when the spaces are the same. For a given linear operator  $A \in \mathcal{L}(\mathcal{Y}_0, \mathcal{Y}_1)$ ,  $A^\#$  denotes its adjoint and for  $N \in \mathbb{N}^*$ ,  $A_{(N)} \in \mathcal{L}(\mathcal{Y}_0^N, \mathcal{Y}_1^N)$  denotes the operator  $A_{(N)} : (y_0^1, \dots, y_0^N) \mapsto (Ay_0^1, \dots, Ay_0^N)$ . For two matrices  $B_0 \in \mathbb{R}^{m \times p}$ ,  $B_1 \in \mathbb{R}^{n \times q}$ ,  $B_0 \otimes B_1 \in \mathbb{R}^{m \times p \times q}$  denotes their Kronecker product. Finally  $L^2(\Theta)$  denotes the Hilbert space of equivalence classes of square integrable functions on a given compact subset  $\Theta \subset \mathbb{R}^q$ .

## 2 A general approach to functional regression

### 2.1 Exact functional learning problem

Let  $\mathcal{X}$  be an input set and let  $\mathcal{Y} \subset L^2(\Theta)$  be the output space. Let  $(X, Y)$  be a couple of random variables on  $\mathcal{X} \times \mathcal{Y}$  distributed according to  $P_{X, Y}$ , a fixed yet unknown probability distribution. We observe  $N \in \mathbb{N}^*$  realizations of these random variables  $\mathcal{S}_N := (x_i, y_i)_{i=1}^N$ . In this section as well as Section 3, we consider the so-called *Dense Functional Data Analysis setting* Kokoska & Reimherr (2017) in which each realization of the output functional variable is assumed to be fully observed in  $\Theta$ , whereas *Sparse Functional Data Analysis setting* Kokoska & Reimherr (2017); Li & Hsing (2010); Cai & Yuan (2011) corresponds to practical situations where the sampling grid of the output signal is not so fine and/or irregular.

We denote by  $\ell$  the quadratic loss defined on  $L_2(\Theta) \times L_2(\Theta)$  as  $\ell(y_0, y_1) = \|y_0 - y_1\|_{L_2(\Theta)}^2$ . We consider as well an hypothesis set  $\mathcal{G} \subset \mathcal{F}(\mathcal{X}, \mathcal{Y})$  over which we want to minimize the expected risk, defined for  $g \in \mathcal{G}$  as:

$$\mathcal{R}(g) := \mathbb{E}_{X, Y} [\ell(Y, g(X))]. \quad (1)$$

However, we do not have access to it directly, so we use its empirical counterpart

$$\widehat{\mathcal{R}}(g, \mathcal{S}_N) := \frac{1}{N} \sum_{i=1}^N \ell(y_i, g(x_i)). \quad (2)$$

In practice to avoid overfitting, a regularization penalty can be added to this empirical risk yielding a problem of the form

$$\min_{g \in \mathcal{G}} \widehat{\mathcal{R}}(g, \mathcal{S}_N) + \lambda \Omega_{\mathcal{G}}(g), \quad (3)$$

where  $\Omega_{\mathcal{G}} : \mathcal{G} \mapsto \mathbb{R}_+^*$  is a penalty function that measures the complexity of  $g$  and  $\lambda > 0$  is a real hyperparameter.

## 2.2 Approximation of a signal with dictionaries

In the following, we propose to solve the Functional-Output Regression problem depicted in Eq. (3) by focusing on representations of functional outputs in terms of elementary signals. The idea is to approximate any function  $y$  belonging to the output space  $\mathcal{Y}$  with a linear combination of the form  $\sum_{d=1}^D c_d \phi_d$ , where  $\phi := (\phi_d)_{d=1}^D \in \mathbf{L}^2(\Theta)^D$  with  $D \in \mathbb{N}^*$ . We now refer to the finite family  $\phi$  as the *dictionary*. We denote  $\text{Span}(\phi_1, \dots, \phi_D)$  the space of linear combinations of functions of  $\phi$ .

In the sequel, we need to relate the  $\mathbf{L}^2(\Theta)$  norm of any  $g \in \text{Span}(\phi_1, \dots, \phi_D)$  to the  $\ell^2$  norm of its coefficients in the dictionary  $\phi$ . To this end, a usual assumption on  $\phi$  is that it is a *Riesz family* Casazza (2000) :

**Definition 2.1. (Riesz family and frame)** The dictionary  $\phi := (\phi_d)$  is said to be a Riesz family of  $\mathbf{L}^2(\Theta)$  with lower constant  $c_\phi$  and upper constant  $C_\phi$  if for any  $\gamma = (\gamma_d) \in \mathbb{R}^D$ , one has

$$c_\phi \|\gamma\|_{\mathbb{R}^D} \leq \left\| \sum_{d=1}^D \gamma_d \phi_d \right\|_{\mathbf{L}^2(\Theta)} \leq C_\phi \|\gamma\|_{\mathbb{R}^D} . \quad (4)$$

If in addition each function  $\phi_d$  of the dictionary has unit norm :  $\forall d \in \{1, \dots, D\}, \|\phi_d\|_{\mathbf{L}^2(\Theta)} = 1$ , it is said to be a *normed* Riesz family.

If the dictionary  $\phi := (\phi_d)$  is a Riesz family, it is also a *frame* of  $\text{Span}(\phi_1, \dots, \phi_D)$  with lower constant  $c_\phi^2$  and upper constant  $C_\phi^2$ —see Proposition 4.3 of Casazza (2000)—, that is :  $\forall f \in \text{Span}(\phi_1, \dots, \phi_D)$ ,

$$c_\phi^2 \|f\|_{\mathbf{L}^2(\Theta)}^2 \leq \sum_{d=1}^D \langle f, \phi_d \rangle^2 \leq C_\phi^2 \|f\|_{\mathbf{L}^2(\Theta)}^2 . \quad (5)$$

The dictionary  $\phi$  can be preselected among some specified family of functions, for e.g. splines Oswald (1990) or wavelets DeVore et al. (1992) that have proved their efficiency in signal compression, or it can be learned from the training set to get a sparse representation of data. In the sequel, we assume that the dictionary  $\phi$  is fixed and known in advance. The choice of the dictionary is an important one and may depend on the nature of the data. We give more insights on this question in Section 5. Learning the dictionary is however left for future works.

To define properly our problem and formalize our learning procedure, we introduce the following projection operator :

**Definition 2.2. Projection operator** We define  $\Phi$  as the projection operator associated with the dictionary  $\phi$  of size  $D$ . When applied to a vector  $u \in \mathbb{R}^D$  it provides the linear combination of functions  $\phi_d$ 's weighted by  $u$ .

$$\Phi : u \in \mathbb{R}^D \longmapsto \sum_{d=1}^D u_d \phi_d \in \mathbf{L}^2(\Theta)$$

We can give an explicit expression of  $\Phi^\#$

**Lemma 2.1.** *The adjoint of  $\Phi$  is given by:*

$$\begin{aligned} \Phi^\# : \mathbf{L}^2(\Theta) &\longrightarrow \mathbb{R}^D \\ g &\longmapsto (\langle \phi_d, g \rangle_{\mathbf{L}^2(\Theta)})_{d=1}^D . \end{aligned}$$

Hence  $\Phi^\# \Phi \in \mathcal{L}(\mathbb{R}^D)$  can be represented by the following matrix

$$\Phi^\# \Phi = (\langle \phi_d, \phi_{d'} \rangle_{\mathbf{L}^2(\Theta)})_{d, d'=1}^D . \quad (6)$$

### 2.3 Approximated Functional Regression problem on a dictionary

We now explain how to use an approximation of the output signal with the dictionary  $\phi$  to derive from Eq. (3) an approximated Functional Regression problem associated to  $\phi$ . We propose a new framework for Functional Regression which we call *Projection Learning* based on a given dictionary  $\phi$ . The core idea is to solve the problem depicted in Eq. (3) using a much simpler model defined as  $g(x) = \Phi h(x), \forall x \in \mathcal{X}$ , where  $h : \mathcal{X} \rightarrow \mathbb{R}^D$  is a  $D$ -dimensional vector-valued function.

Learning a model of this form to address the problem in Eq. (3) boils down to solving the approximated problem

$$\min_{h \in \mathcal{H}} \frac{1}{N} \sum_{i=1}^N \ell(y_i, \Phi h(x_i)) + \lambda \Omega_{\mathcal{H}}(h), \quad (7)$$

where  $\mathcal{H} \subset \mathcal{F}(\mathcal{X}, \mathbb{R}^D)$  and the function  $\Omega_{\mathcal{H}} : \mathcal{H} \rightarrow \mathbb{R}$  is a given regularization function. In other words, we search a solution to Eq.(7) in the hypothesis space  $\mathcal{G}_{\mathcal{H},\phi} := \{g : x \mapsto \Phi h(x) \mid h \in \mathcal{H}\}$  paying however the price solving the problem in a space of vector-valued functions  $\mathcal{H}$ . *Projection Learning* therefore combines a representation of the functional output  $g \in \mathcal{G}_{\mathcal{H},\phi}$  on a dictionary with the minimization of a functional loss  $\ell$ .

We emphasize, that to the best of our knowledge this framework is new. Existing dictionary-based approaches—see for instance [Oliva et al. \(2015\)](#)—are based on a two-step strategy : one first approximates the functional output on a finite dictionary, and thereafter solves the remaining vectorial regression problem. With *Projection Learning*, even though the hypothesis class consists of vector-valued functions, the loss remains a functional one. Moreover, any predictive model devoted to vectorial outputs regression (neural networks, random forests, kernel methods) is eligible in this setting. Nevertheless this new framework raises several interesting questions, in particular those of regularization. Indeed, the nature of the regularization has changed in Eq. (7) compared to Eq. (3) since  $\Omega_{\mathcal{H}}$  now controls the vectorial output function  $h$ . A relevant question is how to convey interesting properties on the output function  $\theta \rightarrow \sum_{d=1}^D \phi_j(\theta) h_d(x)$  for a given  $x$  through the predicted coefficients  $h_d(x)$  on the dictionary.

In Section 3, we therefore focus on Kernel-based Projection learning (KPL), based on the general framework of vector-valued Reproducing Kernel Hilbert Spaces.

## 3 Projection Learning with vv-RKHS.

### 3.1 Projection learning with vv-RKHS

Let  $\mathsf{K} : \mathcal{X} \times \mathcal{X} \mapsto \mathcal{L}(\mathbb{R}^D)$  be an OVK with  $\mathcal{H}_{\mathsf{K}} \subset \mathcal{F}(\mathcal{X}, \mathbb{R}^D)$  its associated vv-RKHS. We consider Eq. (7) with the vector-valued hypothesis class  $\mathcal{H}$  set as  $\mathcal{H}_{\mathsf{K}}$ . We introduce the following shorter notation for the set  $\mathcal{G}_{\mathcal{H}_{\mathsf{K}},\phi}$  denoted as  $\mathcal{G}_{\mathsf{K},\phi} := \mathcal{G}_{\mathcal{H}_{\mathsf{K}},\phi}$ . Setting the regularization on  $\mathcal{H}_{\mathsf{K}}$  as  $\Omega_{\mathcal{H}_{\mathsf{K}}}(h) := \|h\|_{\mathcal{H}_{\mathsf{K}}}^2$  yields the following instantiation of *Projection learning* with vv-RKHS:

$$\min_{h \in \mathcal{H}_{\mathsf{K}}} \frac{1}{N} \sum_{i=1}^N \ell(y_i, \Phi h(x_i)) + \lambda \|h\|_{\mathcal{H}_{\mathsf{K}}}^2. \quad (8)$$

### 3.2 Resolution with representer theorem

Eq. (8) however involves solving an optimization problem in an infinite dimensional space  $\mathcal{H}_{\mathsf{K}}$ . It can nevertheless be restated in finite dimension with  $ND$  variables. This is the object of Proposition 3.1 which is an analogous to the well known Representer theorem.

**Proposition 3.1. (Representer theorem)** *If  $\ell$  is continuous and convex with respect to its second argument, the problem in Eq. (8) admits a unique minimizer  $\widehat{h}_{\mathcal{S}_N}$ . Moreover there exist  $(\alpha_j)_{j=1}^N \in \mathbb{R}^D$  such that*

$$\widehat{h}_{\mathcal{S}_N} = \sum_{j=1}^N \mathbf{K}(\cdot, x_j) \alpha_j .$$

**Sketch of proof.** *We use strict convexity for existence and unicity of the minimizer  $\widehat{h}_{\mathcal{S}_N}$ . Then we use orthogonal projection to show that writing  $\widehat{h}_{\mathcal{S}_N} = \sum_{j=1}^N \mathbf{K}(\cdot, x_j) \alpha_j$  does not changes the value of the data-fitting term yet decreases the regularization term. The fully detailed proof is in the Subsection B.1 Supplementary.*

By Proposition 3.1, if the loss function  $\ell$  is the quadratic loss in  $\mathbf{L}^2(\Theta)$ , the problem in Eq. (8) becomes

$$\begin{aligned} \min_{\alpha_1, \dots, \alpha_N \in \mathbb{R}^D} \frac{1}{N} \sum_{i=1}^N \left\| y_i - \Phi \sum_{j=1}^N \mathbf{K}(x_i, x_j) \alpha_j \right\|_{\mathbf{L}^2(\Theta)}^2 \\ + \lambda \sum_{i,j=1}^N \langle \alpha_i, \mathbf{K}(x_i, x_j) \alpha_j \rangle_{\mathbb{R}^D} , \end{aligned} \quad (9)$$

which can be rewritten as

$$\min_{\alpha \in \mathbb{R}^{DN}} \frac{1}{N} \left\| \mathbf{y} - \Phi_{(N)} \mathbf{K} \alpha \right\|_{\mathbf{L}^2(\Theta)^N}^2 + \lambda \langle \alpha, \mathbf{K} \alpha \rangle_{\mathbb{R}^{DN}} . \quad (10)$$

Where  $\mathbf{y} := (y_i)_{i=1}^N \in \mathbf{L}^2(\Theta)^N$ ,  $\Phi_{(N)} : \mathbb{R}^{DN} \rightarrow \mathbf{L}^2(\Theta)^N$  is block scalar—see notations at the end of Sec. 1—and the kernel matrix  $\mathbf{K} \in \mathbb{R}^{DN \times DN}$  is defined block-wise by

$$\mathbf{K} := \begin{bmatrix} K(x_1, x_1) & \dots & K(x_1, x_N) \\ \vdots & \ddots & \vdots \\ K(x_N, x_1) & \dots & K(x_N, x_N) \end{bmatrix}$$

We now provide an explicit solution for the problem (10).

**Proposition 3.2. (Closed form solution)** *The minimum of the problem in Eq. (10) is achieved by any  $\alpha^*$  satisfying*

$$(\mathbf{K}(\Phi^\# \Phi)_{(N)} \mathbf{K} + N \lambda \mathbf{K}) \alpha^* := \mathbf{K} \Phi_{(N)}^\# \mathbf{y} , \quad (11)$$

*which has at least one solution  $\alpha^* \in \mathbb{R}^{DN}$ . Moreover if  $\mathbf{K}$  is full rank then  $((\Phi^\# \Phi)_{(N)} \mathbf{K} + N \lambda \mathbf{K})$  is invertible and*

$$\alpha^* := ((\Phi^\# \Phi)_{(N)} \mathbf{K} + N \lambda \mathbf{K})^{-1} \mathbf{K} \Phi_{(N)}^\# \mathbf{y} . \quad (12)$$

Note that  $(\Phi^\# \Phi)_{(N)}$  is a block diagonal matrix with the Gram matrix  $\Phi^\# \Phi$  defined in Eq. (6) repeated on its diagonal.

**Sketch of proof.** *The problem in Eq. (10) is a quadratic form in  $\alpha$ . Using the adjoint  $\Phi_{(N)}^\#$  of  $\Phi_{(N)}$ , we can express it in terms of scalar products in  $\mathbb{R}^{DN}$ . Minimizing the obtained quadratic form involves the block diagonal operator  $(\Phi^\# \Phi)_{(N)}$ . The obtained explicit solution benefits from the fact that the operator  $\mathbf{K}$  cancels out. The fully detailed proof is in the Subsection B.2 of the Supplementary.*

### 3.3 Bound on estimation error

We define the space  $\mathcal{H}_\kappa(a) := \{h \in \mathcal{H}_\kappa, \|h\|_{\mathcal{H}_\kappa} \leq a\}$  with  $a > 0$ . We highlight that  $\forall \lambda > 0, \exists a > 0$  such that the problem in Eq. (8) is equivalent to minimizing the empirical risk only over  $\mathcal{H}_\kappa(a)$  and conversely. We now consider  $a$  given. The loss  $\ell$  is still the quadratic loss on  $L^2(\Theta)$ . We make the following assumptions:

**Assumption 3.1.**  $\mathcal{Y}$  is bounded:  $\exists c_Y \in \mathbb{R}, \forall y \in \mathcal{Y}, \|y\|_{L_2(\Theta, \mu)} \leq c_Y$ .

**Assumption 3.2.** The kernel is bounded in the sense of its operator norm:  $\exists c_K \in \mathbb{R}, \forall x \in \mathcal{X}, \|\mathbf{K}(x, x)\|_{O_p} \leq c_K$ .

*Remark.* Let  $D \in \mathbb{N}^*$ , and  $\mathbf{K}^D : \mathcal{X} \times \mathcal{X} \rightarrow \mathbb{R}^{D \times D}$  and OVK. If for all  $x \in \mathcal{X}, \mathbf{K}^D(x, x)$  is composed only of blocks which sizes do not depend on  $D$ , then we can suppose that  $c_{\mathbf{K}^D}$  does not depend on  $D$ .

**Assumption 3.3.** The dictionary  $\phi$  is a normed Riesz family in  $L^2(\Theta)$  with lower and upper constants  $c_\phi$  and  $C_\phi$ .

**Proposition 3.3. (Bound on estimation error)** Suppose that Assumptions 3.1, 3.2 and 3.3 hold. Let  $\hat{h}_{\mathcal{S}_N}^{(a)} := \arg \min_{h \in \mathcal{H}_\kappa(a)} \hat{\mathcal{R}}(\Phi h, \mathcal{S}_N)$ . Then, we have for any  $\delta > 0$ , with probability  $1 - \delta$ :

$$\begin{aligned} & \mathcal{R}(\Phi \hat{h}_{\mathcal{S}_N}^{(a)}) - \inf_{h \in \mathcal{H}_\kappa(a)} \mathcal{R}(\Phi h) \\ & \leq 8\sqrt{2}a C_\phi (c_Y \sqrt{c_K} + a c_K C_\phi) \frac{\sqrt{D}}{\sqrt{N}} \\ & \quad + 6\sqrt{2}(c_Y^2 + a^2 C_\phi^2 c_K + 2a c_Y C_\phi \sqrt{c_K}) \sqrt{\frac{\log(\frac{4}{\delta})}{N}}. \end{aligned}$$

**Sketch of proof.** We proceed in two steps. Firstly, we adapt the classical proof technique of Theorem 8 in [Bartlett & Mendelson \(2002\)](#) to bound the estimation error in terms of Rademacher complexity, which we in turn bound by the empirical Rademacher complexity. Secondly we bound the latter using the vector concentration inequality of [Maurer \(2016\)](#) combined with properties of our hypothesis class. The fully detailed proof is in the Subsection B.3 of the Supplementary.

We highlight that this bound on estimation error has a dependence in  $N$  of order  $\mathcal{O}(1/\sqrt{N})$  and a dependence in the dimension of the dictionary of  $\mathcal{O}(\sqrt{D})$ .

### 3.4 Implementation with sparsely observed functions.

In practice, we never observe functions but rather discrete observations. We propose next an algorithm for our method which deals directly with such discretized functions and can thus accommodate both sparse and dense functional analysis problems without the need to perform smoothing beforehand. From now on we suppose that the domain of the output functions is unidimensional, which is in practice the most frequent setting in FDA. Without loss of generality we then set  $\Theta = [0, 1]$ , since any interval of  $\mathbb{R}$  in can be renormalized to fit into this framework.

**Definition 3.1. Sparse functional sample** A sparse functional response sample of size  $N$  is defined as a set of observations of the form

$$\mathcal{S}_N^{\text{obs}} := \left( \left( x_i, (\theta_{im}, y_{im}^{\text{obs}})_{m=1}^{M_i} \right) \right)_{i=1}^N,$$

with for all  $i \in [N], M_i \in \mathbb{N}^*$  corresponds to the number of discretization points available for the  $i$ -th function, and for all  $i \in [N]$  and  $m \in [M_i], \theta_{im} \in \Theta$  and  $y_{im}^{\text{obs}} \in \mathbb{R}$ .

In the closed form solution of Eq. (12), the functions  $\mathbf{y} = (y_i)_{i=1}^N$  only appear through the quantity  $(\Phi_{(N)})^\# \mathbf{y} = [\Phi^\# y_1, \dots, \Phi^\# y_N] \in \mathbb{R}^{ND}$ , and for all  $i \in N$ ,  $\Phi^\# y_i = (\langle y_i, \phi_d \rangle_{L^2(\Theta)})_{d=1}^D$ . We introduce as well the notation  $\eta_{id} := \langle y_i, \phi_d \rangle_{L^2(\Theta)}$ . We can estimate those scalar products from the sample  $\mathcal{S}_N^{\text{obs}}$  as:

$$\hat{\eta}_{id} := \frac{1}{M_i} \sum_{m=1}^{M_i} y_{im}^{\text{obs}} \phi_d(\theta_{im}) . \quad (13)$$

For all  $i$  we define  $\hat{\eta}_i := (\hat{\eta}_{id})_{d=1}^D \in \mathbb{R}^D$  and  $\hat{\boldsymbol{\eta}} \in \mathbb{R}^{ND}$  the vector obtained by concatenating the vectors  $(\eta_i)_{i=1}^N$ . We can then replace  $(\Phi_{(N)})^\# \mathbf{y}$  in Eq. (11) by its estimate  $\hat{\boldsymbol{\eta}}$ .

**Choice of kernels.** When dealing with RKHS, the choice of the kernel directly influences the kind of regularization conveyed by the RKHS norm. In practice, the separable kernel is often used. It is of the form  $\mathbf{K} : (x_0, x_1) \mapsto k(x_0, x_1) \mathbf{B}$  Alvarez et al. (2012), with  $k$  a scalar kernel on  $\mathcal{X}$  and  $\mathbf{B} \in \mathbb{R}^{D \times D}$  a positive semi-definite matrix. Its coefficients encode how the output coordinates relate. In our setting, if we have a prior information about the nature of the decomposition on a given dictionary, we can thus express it through  $\mathbf{B}$ . Even a simple diagonal matrix can be relevant, allowing for instance to give more importance to some basis functions given their frequency for a Fourier dictionary or given their scale for wavelets dictionaries. We exploit this in the numerical experiments related to biomedical imaging in subsection 5.2 using wavelets. We however leave kernel learning for future works.

**Fast implementation with separable kernels.** In this separable kernel case, the kernel matrix  $\mathbf{K}$  can be rewritten as  $\mathbf{K} = \mathbf{K}_{\mathcal{X}} \otimes \mathbf{B}$  with  $\mathbf{K}_{\mathcal{X}} \in \mathbb{R}^{N \times N}$  the kernel matrix associated with the scalar kernel  $k$ . Computing the closed form of Eq. 11 is too complex—time complexity of  $\mathcal{O}(N^3 D^3)$ —, however, we can write  $(\Phi_{(N)})^\# \Phi_{(N)} = \mathbf{I} \otimes (\Phi^\# \Phi)$ . Thus  $(\Phi_{(N)})^\# \Phi_{(N)} \mathbf{K} = (\mathbf{I} \otimes (\Phi^\# \Phi)) (\mathbf{K}_{\mathcal{X}} \otimes \mathbf{B})$ . Using the mixed product property of the Kronecker product—Lemma 4.2.10 in Horn & Johnson (1991)—, we must then find a solution to the system

$$(\mathbf{K}_{\mathcal{X}} \otimes ((\Phi^\# \Phi) \mathbf{B}) + N\lambda \mathbf{I}) \boldsymbol{\alpha} = \hat{\boldsymbol{\eta}} .$$

As highlighted in the Subsection 4.1 in Dinuzzo et al. (2011), such system can be formulated as a discrete time Sylvester equation Sima (1996).

Solving such system has time complexity  $\mathcal{O}(N^3 + D^3 + N^2 D + ND^2)$ . In practice we use two Python packages <sup>1 2</sup> which gives acces in Python to the routines of the library SLICOT <sup>3</sup>. The steps required to fit our method either from sparsely or densely observed functions are summed up in Algorithm 1. Once an  $\boldsymbol{\alpha}^*$  has been found, given a new set of inputs  $(x_i^{\text{new}})_{i=1}^{N_{\text{new}}}$ , we compute the scalar new kernel matrix  $\mathbf{K}_{\mathcal{X}}^{\text{new}} := (k(x_i, x_j^{\text{new}}))_{i=1, j=1}^{N, N_{\text{new}}} \in \mathbb{R}^{N \times N_{\text{new}}}$  prediction of the projection coefficients on the dictionary are the columns of the matrix  $\mathbf{B} \mathbf{mat}(\boldsymbol{\alpha}^*) \mathbf{K}_{\mathcal{X}}^{\text{new}} \in \mathbb{R}^{D \times N_{\text{new}}}$ , where  $\mathbf{mat}(\boldsymbol{\alpha}^*) \in \mathbb{R}^{D \times N}$  is the matrix obtained by slicing  $\boldsymbol{\alpha}^*$  in  $N$  vectors of size  $D$  and then stacking them as columns to form a matrix.

## 4 Related works

We present emblematic works for four types of approaches to non-linear functional-output regression: a nonlinear kernel-based extension Reimherr & Sriperumbudur (2017) of functional

---

<sup>1</sup>www.pypi.org/project/slycot/

<sup>2</sup>www.python-control.readthedocs.io/

<sup>3</sup>www.slicot.org



---

**Algorithm 1** Algorithm with separable kernel

---

**Input:** data  $\mathcal{S}_N^{\text{obs}}$ , matrices  $\mathbf{B}$ ,  $\Phi^\# \Phi$   
**Compute:** kernel matrix  $\mathbf{K}_{\mathcal{X}} = (k(x_i, x_j))_{i,j=1}^N$   
**Compute:** estimates  $\hat{\boldsymbol{\eta}}$  of  $(\langle y_i, \phi_d \rangle_{\mathcal{L}^2(\Theta)})_{i=1, d=1}^{N, D}$  using Eq. (13).  
**Solve:**  $(\mathbf{K}_{\mathcal{X}} \otimes ((\Phi^\# \Phi) \mathbf{B}) + N\lambda) \boldsymbol{\alpha} = \hat{\boldsymbol{\eta}}$  with Sylvester solver.

---

linear models Ramsay & Silverman (2005), a Functional Kernel Ridge Regression approach Kadri et al. (2016), a functional extension of the celebrated Nadaraya-Watson kernel estimator Ferraty et al. (2011) and the Triple-Basis Estimator (3BE) Oliva et al. (2015). We have re-implemented and compare them with our method in Section 5. Note that at the exception of that of Reimherr & Sriperumbudur (2017) which only accepts function inputs, all the other methods can deal with any input type, including 3BE which can also takes as input a feature vector instead of the coefficients of expansion.

Reimherr & Sriperumbudur (2017) build on the Additive Function-on Function Regression model leveraging RKHSs. Considering the domain of both input and output functions to be  $[0, 1]$ , they solve the regularized empirical problem

$$\min_{g \in \mathcal{H}_\kappa} \sum_{i=1}^N \int_0^1 \left( y_i(t) - \int_0^1 g(t, s, x_i(s)) ds \right)^2 dt + \lambda \|g\|_{\mathcal{H}_\kappa}^2,$$

where  $\mathcal{H}_\kappa$  is a the RKHS associated to some kernel  $\kappa : ([0, 1] \times [0, 1] \times \mathbb{R})^2 \rightarrow \mathbb{R}$  and  $\lambda > 0$ . A Representer Theorem applies and the use of the squared loss leads to closed-form solution. To alleviate the computations, the solution is expressed in the truncated basis of dimension  $J < N$  of empirical functional principal components of  $y_1, \dots, y_N$ . The complexity in time reduces to inverting a  $NJ \times NJ$  matrix. We refer to this approach as **Kernel Additive Model (KAM)**.

Kadri et al. (2016) proposes to extend the kernel ridge regression problem to function-on-function regression using the general framework of operator-valued kernels and function-valued Reproducing Kernel Hilbert Spaces.

$$\min_{g \in \mathcal{H}_\kappa} \sum_{i=1}^N \|y_i - g(x_i)\|_{\mathcal{Y}}^2 + \lambda \|g\|_{\mathcal{H}_\kappa}^2,$$

When focusing on a separable kernel  $\mathbf{K}(x_0, x_1) = k(x_0, x_1)T$  with  $k$ , a scalar-valued kernel and  $T$  an operator of  $\mathcal{L}(\mathcal{Y})$ , then the full OVK rewrites  $\mathbf{K} = \mathbf{K}_{\mathcal{X}} \otimes T$  and the problem can be solved using a (truncated) spectral decomposition of the Gram matrix  $\mathbf{K}_{\mathcal{X}}$  of the scalar kernel  $k$  and of the operator  $T$ . Typically if  $J < N$  is the number of eigenfunctions, this approach boils down to inverting a  $NJ \times NJ$  matrix. We refer to this approach as **Functional Kernel Ridge Regression (FKRR)**.

Yet another nonparametric approach—which we refer to as **Kernel Estimator (KE)**—, the functional Nadaraya-Watson kernel estimator, has been studied in Ferraty et al. (2011) in the general setting of Banach spaces. A simple version of this estimator can however be given. Considering a kernel function  $K : \mathbb{R} \mapsto \mathbb{R}$  combined with a given semi-metric  $S$  on  $\mathcal{X}$ , the estimator is

$$g(x) := \frac{\sum_{i=1}^N K \circ S(x, x_i) y_i}{\sum_{i=1}^N K \circ S(x, x_i)}.$$

Finally, Oliva et al. (2015) adopt another angle. They firstly represent separately the input and output functions on truncated orthonormal bases. In doing so they obtain a set of input and

output decomposition coefficients  $(\beta_i, \gamma_i)_{i=1}^N$  with for all  $i \in [N]$ ,  $\beta_i \in \mathbb{R}^P$  and  $\gamma_i \in \mathbb{R}^D$ ,  $P \in \mathbb{N}^*$  being the dimension in the input basis and  $D \in \mathbb{N}^*$  that of the output basis. They then perform approximate kernel ridge regressions using Random Fourier Features [Rahimi & Recht \(2008\)](#) to regress the output coefficients on the input ones. Even though it represents technically  $D$  distinct sub-problems, since the inputs are the same, using the closed form for the ridge regression, only one matrix inversion step has to be performed. Putting aside the computations of the decomposition coefficients, this yields a complexity of  $\mathcal{O}(J^3)$  with  $J$  the number of Random Fourier Features used. We refer to this approach as **Triple Basis Estimator (3BE)**.

## 5 Experiments

We firstly test the robustness of our method on a toy dataset in Subsection 5.1, thereafter we compare it with the four other state-of-the-art methods presented in Section 4 on two datasets with different characteristics. In Subsection 5.2 we explore a biomedical imaging dataset with relatively small  $N = 100$  and sparsely observed output functions, whereas in Subsection 5.3 we study a speech inversion dataset with relatively large  $N = 413$  and densely observed output functions.

Throughout this section, we use the mean squared error (MSE) as metric. For a given sample sparse functional sample  $\mathcal{S}_N^{\text{obs}}$ —see 3.1—on which we want to evaluate a set of predicted functions  $(\hat{y}_i)_{i=1}^N \in \mathcal{L}^2(\Theta)$  we measure the error as

$$\text{MSE} := \frac{1}{N} \sum_{i=1}^N \frac{1}{M_i} \sum_{m=1}^{M_i} (\hat{y}_i(\theta_{im}) - y_{im}^{\text{obs}})^2$$

For simplicity’s sake we do not give the full details of parameters and tuning processes, such details are however given in the Section C of the Supplementary.

### 5.1 Toy data

In all the experiments in this subsection, we use the separable kernel  $\mathbb{K}(x_0, x_1) := k(x_0, x_1)$  with  $k$  a scalar-valued Gaussian kernel. We use a toy dataset that we generate. Essentially, to a random mixture of trigonometric functions with random frequencies, we associate a mixture of localized functions—we use cubic B-splines [de Boor \(2001\)](#) centered at the corresponding frequencies. The full generating process for this dataset is described in the Supplementary Subsection C.1.

**Robustness to noise.** In this first experiment, we focus on the effect of a first type of corruption of the output function. To this end, we add a Gaussian noise to our outputs. We consider a training set of  $N_{\text{train}} = 500$  train samples and  $N_{\text{test}} = 300$  test samples. We consider 50 Gaussian noise levels characterized by their standard deviations ranging from  $\sigma_y = 0$  to  $\sigma_y = 1.5$ . For each level, we cross validate the regularization parameter. The evolution of the scores on the test set are shown in Figure 1. We used as x-axis the signal to noise ratio which we define for a given noise level  $\sigma_y$  and from an observed sample  $\mathcal{S}_N^{\text{obs}}$ —see Definition 3.1—as  $\text{SNR} := \frac{\frac{1}{N} \sum_{i=1}^N \frac{1}{M_i} \sum_{m=1}^{M_i} |y_{im}^{\text{obs}}|}{\sigma_y}$ .

**Robustness to missing data.** In this second experiment, we focus on missing values. We keep a fixed level of output noise with  $\sigma_y = 0.07$ , however we now remove as well uniformly at random a given percentage of the evaluations for each training output function. We do so on a grid ranging from 0 % to 90 % of evaluations missing. We repeated the experiments for several number of training samples size. At each run we cross validate the regularization parameter. The results are shown in Fig. 2.

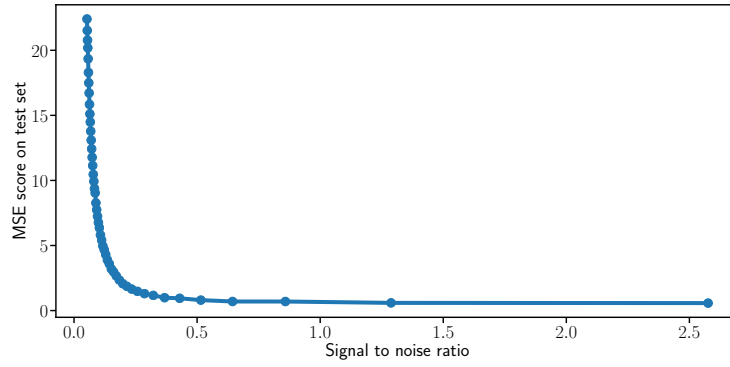


Figure 1: Robustness to output noise on splines toy dataset with  $N = 500$  samples.

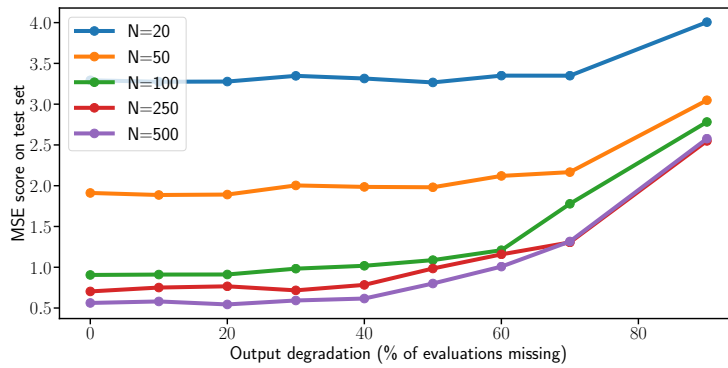


Figure 2: Robustness to random missing evaluations in the outputs functions for several number of samples  $N$ .

Table 1: Comparison of nonlinear functional-output regression methods on the DTI dataset.

	KE	3BE	KPL	KAM	FKRR
MSE <sub>TEST</sub>	0.251	0.249	<b>0.233</b>	0.242	0.238

## 5.2 Diffusion Tensor Imaging Data (DTI)

**Dataset.** We now consider a Diffusion Tensor Imaging dataset <sup>1</sup>. This dataset was collected at Johns Hopkins University and the Kennedy-Krieger Institute. It consists of two Fractional anisotropy (FA) profiles inferred from the DTI scans. They are given along two tracts—the corpus callosum (CCA) and the right corticospinal (RCS) one. It contains 382 such profiles from 142 subjects, 100 subjects suffering from multiple sclerosis (MS) and 42 healthy controls. MS is an auto-immune disease which causes the immune system to gradually destroy myelin. This process is however not spatially uniform and not well understood. Thus, using the proxy of FA profiles, we propose to predict one tract (RCS) from the other (CCA). So as to remain in an i.i.d framework, we consider only the first scans of MS patients resulting in  $N = 100$  pairs of functions. We highlight that the output functions have a lot of missing values with whole chunks sometimes missing.

**Experimental setting.** Since very few values are missing for the input functions, we used linear interpolation yielding regularly observed inputs. However, because of the higher number of missing values in the output functions, we did not perform such interpolation when it was not necessary—for KPL, 3BE et KE. However FKRR and KAM need densely observed functions, so we performed smoothing using linear interpolation. We used  $N_{\text{train}} = 70$  data points for training and  $N_{\text{test}} = 30$  data points for testing. Finally, when using wavelets as dictionary, we extended the signal symmetrically to avoid boundary effects. We now comment on the results shown in Table 1.

**Comments on the results.** For this dataset, all the methods show approximately equivalent MSE with a slight advantage for ours. An efficient use of wavelet bases may explain this difference, as such bases can better accommodate non-smooth data. We did not manage to exploit such advantage with 3BE which performed better with pure Fourier. It may be because KPL performs the smoothing on the output basis conditionally on the input data as opposed to 3BE which performs it independently. We used as well a penalization of scales corresponding to higher frequencies, indeed we took a separable kernel  $K(x_0, x_1) = k(x_0, x_1)D$  with  $k$  a Gaussian kernel and  $D$  a diagonal matrix of weights decreasing with the scale of the wavelet which contributes to the better performance.

## 5.3 Synthetic speech inversion dataset

**Dataset.** Comments on the results. This object of this dataset is to study the speech inversion problem. From a given acoustic speech signal, the aim is to estimate the underlying vocal tract configuration that produced it [Richmond \(2002\)](#). It is motivated for instance by the improvement of the performance of speech recognition systems or to improve speech synthesis. The dataset was introduced by [Mitra et al. \(2009\)](#), it is generated by a software which synthesizes words from an articulatory model. It consists of a corpus of  $N = 413$  pronounced words with 8 distinct vocal tract functions—lip aperture (LA), lip protrusion (LP), tongue tip constriction degree

---

<sup>1</sup>This dataset is freely available as a part of the *Refund* R package

Table 2: Comparison of nonlinear functional regression methods on the synthetic speech dataset

	KE	3BE	KPL	FKRR
LA	9.699	<b>5.730</b>	<b>5.730</b>	5.780
LP	16.096	6.643	6.643	<b>6.641</b>
TTCD	14.381	6.450	6.450	<b>6.447</b>
TTCL	15.742	6.701	6.701	<b>6.658</b>
TBCD	10.946	5.793	5.793	<b>5.791</b>
TBCL	14.027	5.134	5.134	<b>5.132</b>
VEL	14.774	8.584	8.584	<b>8.583</b>
GLO	10.680	<b>4.102</b>	<b>4.102</b>	4.104
AVERAGE	13.2931	6.1421	6.1421	<b>6.1420</b>

(TTCD), tongue tip constriction location (TTCL), tongue body constriction degree (TBCD), tongue body constriction location (TBCL), Velum (VEL) and Glottis (GLO).

**Experimental setting.** Since the duration of the words vary greatly, we padded symmetrically both the input sound and the 8 output vocal tracts to match the longest word. We represented the input sounds using 13 mel cepstral coefficients (MFCCs) and used  $N_{\text{train}} = 300$  instances for training and  $N_{\text{test}} = 113$  for testing. Finally, we normalized the domain of the output functions to be  $[0, 1]$  and normalized the functions themselves so that they take their values in  $[-1, 1]$ . We used the same input kernel for all the methods consisting of a sum of Gaussian kernels with the same standard deviation parameter on the 13 MFCCs. Finally, we used a dictionary of empirical functional principal components for 3BE et KPL. The results are presented in Tab. 2. **Comments on the results.** Experimental setting Firstly, we highlight that the fact that the 3BE and PL columns are identical is not an error, the scores on test set were identical up to the precision  $10^{-5}$ . Cross validation yielded the same parameters for the two methods. Secondly, our method (KPL) and 3BE are dramatically close to FKRR which has however a much higher time complexity—see Section 4.

## 6 Conclusion

We introduced a novel general framework to address Functional Output Regression. It consists in learning to predict the decomposition of the output function on a dictionary using the input. We proposed Kernel-based Projection learning a method that comes with a theoretical bound on estimation error. The experimental study confirmed the interest and the efficiency of the approach on a toydataset and two real world applications in medical imaging and acoustics, especially when compared to four Functional Regression methods that we re-implemented in the same Python library. The wide set of candidate dictionaries makes the method versatile. A promising research direction concerns kernel learning in order to control the sparsity of the predicted expansions. Dictionary learning can also be examined.

## References

Alvarez, A. M., Rosasco, L., and Lawrence, N. D. Kernels for vector-valued functions: a review. *Foundations and Trends in Machine Learning*, 4(3):195–266, 2012.

- Bartlett, P. L. and Mendelson, S. Rademacher and gaussian complexities: risk bounds and structural results. *Journal of Machine Learning Research*, 3:463–482, 2002.
- Bauschke, H. H. and Combettes, P. L. *Convex Analysis and Monotone Operator Theory in Hilbert Spaces*. Springer, 2017.
- Cai, T. T. and Yuan, M. Optimal estimation of the mean function based on discretely sampled functional data: Phase transition. *The Annals of Statistics*, 39:2330–2355, 2011.
- Carmeli, C., De Vito, E., and Umanita, V. Vector valued reproducing kernel hilbert spaces and universality. *Analysis and Applications*, 8:19–61, 2010.
- Casazza, P. G. The art of frame theory. *Taiwanese journal of mathematics*, 4:129–201, 2000.
- Daubechies, I. and Heil, C. *Ten Lectures on Wavelets*. American Institute of Physics, 1992.
- de Boor, C. *A practical guide to Splines - Revised Edition*. Springer, 2001.
- DeVore, R. A., Jawerth, B., and Popov, V. Compression of wavelet decompositions. *American Journal of Mathematics*, 114(4):737–785, 1992.
- Dinuzzo, F., Ong, C. S., Gehler, P., and Pilonetto, G. Learning output kernels with block coordinate descent. In *Proceedings of ICML 2011*, pp. 49–56, 2011.
- Ferraty, F. and Vieu, P. *Nonparametric functional data analysis*. Springer, 2006.
- Ferraty, F., Laksaci, A., Tadj, A., and Vieu, P. Kernel regression with functional response. *Electron. J. Statist.*, 5:159–171, 2011. doi: 10.1214/11-EJS600.
- Horn, R. A. and Johnson, C. R. *Topics in Matrix Analysis*. Cambridge University Press, 1991.
- Kadri, H., Duflos, E., Preux, P., Canu, S., Rakotomamonjy, A., and Audiffren, J. Operator-valued kernels for learning from functional response data. *Journal of Machine Learning Research*, 17:1–54, 2016.
- Kokoska, P. and Reimherr, M. *Introduction to Functional Data Analysis*. CRC Press, 2017.
- Li, Y. and Hsing, T. Uniform convergence rates for nonparametric regression and principal component analysis in functional/longitudinal data. *The Annals of Statistics*, 38:3321–3351, 2010.
- Lian, H. Nonlinear functional models for functional responses in reproducing kernel hilbert spaces. *Canadian Journal of Statistics*, pp. 597–606, 2007.
- Mallat, S. *A Wavelet Tour of Signal Processing*. Academic Press, 2008.
- Maurer, A. A vector-contraction inequality for rademacher complexities. In *Proceedings of ALT 2016*, pp. 3–17, 2016.
- Meyer, Y. *Wavelets and Operators*. Cambridge University Press, 1993.
- Micchelli, C. A. and Pontil, M. On learning vector-valued functions. *Neural Computation*, 17(1):177–204, 2005.
- Mitra, V., Ozbek, Y., Nam, H., Zhou, X., and Espy-Wilson, C. Y. From acoustics to vocal tract time functions. In *IEEE International Conference on Acoustics, Speech and Signal Processing (ICASSP)*, pp. 4497–4500, 2009.

- Mohri, M., Rostamizadeh, A., and Talwalkar, A. *Foundations of Machine Learning*. The MIT Press, second edition, 2018.
- Morris, J. S. Functional regression. *The Annual Review of Statistics and Its Application*, 2: 321–359, 2015.
- Oliva, J., Neiswanger, W., Poczos, B., Xing, E., Trac, H., Ho, S., and Schneider, J. Fast function to function regression. In *Proceedings of AISTATS 2015*, volume 38, pp. 717–725, 2015.
- Oswald, P. On the degree of nonlinear spline approximation in besov-sobolev spaces. *Journal of approximation theory*, 61(2):131–157, 1990.
- Rahimi, A. and Recht, B. Random features for large-scale kernel machines. In Platt, J. C., Koller, D., Singer, Y., and Roweis, S. T. (eds.), *Advances in Neural Information Processing Systems (NIPS) 20*, pp. 1177–1184. Curran Associates, Inc., 2008.
- Ramsay, J. O. and Silverman, B. W. *Functional data analysis*. Springer, 2005.
- Reimherr, M. and Sriperumbudur, B. Optimal prediction for additive function on function regression. *Electronic Journal of Statistics*, 12:4571–4601, 2017.
- Richmond, K. *Estimating Articulatory Parameters from the Acoustic Speech Signal*. PhD thesis, The Center for Speech Technology Research, Edinburgh University, 2002.
- Senkene, E. and Templeman, A. Hilbert spaces of operator-valued functions. *Lithuanian Mathematical Journal*, 1973.
- Sima, V. *Algorithms for Linear-Quadratic Optimization*. Chapman and Hall/CRC, 1996.

## Appendices

This supplementary Material is organized as follows. Section A provides a reminder about Operator-valued Kernels and vv-RKHS. In Section B, the proofs of all theorems and propositions in the core paper are detailed. Section C shortly describes each dataset and presents the experimental setting, along with the model selection method.

### A A few key properties of vector-valued and function-valued RKHS

First, we give the definition of an Operator-Valued Kernel (OVK) and of its associated Reproducing Kernel Hilbert Space (RKHS).

**Definition A.1.** Let  $\mathcal{X}$  be any space, let  $\mathcal{Y}$  be a Hilbert space, an operator-valued kernel on  $\mathcal{X} \times \mathcal{X}$  is a function  $\mathbb{K} : \mathcal{X} \times \mathcal{X} \rightarrow \mathcal{L}(\mathcal{Y})$  that verifies the two following conditions:

- For all  $x, x' \in \mathcal{X}$ ,  $\mathbb{K}(x, x') = \mathbb{K}(x', x)^\#$ ,
- For all  $N \in \mathbb{N}^*$ , for all  $x_1, \dots, x_N \in \mathcal{X}$ , for all  $y_1, \dots, y_N \in \mathcal{Y}$ ,

$$\sum_{i=1}^N \sum_{j=1}^N \langle y_i, \mathbb{K}(x_i, x_j) y_j \rangle_{\mathcal{Y}} \geq 0 .$$

The following theorem shows that given any operator-valued kernel, it is possible to build a unique reproducing kernel Hilbert space associated to this kernel.

**Theorem A.1.** *Senkene & Templeman (1973); Carmeli et al. (2010)* Given an operator-valued kernel  $\mathbb{K} : \mathcal{X} \times \mathcal{X} \rightarrow \mathcal{L}(\mathcal{Y})$ , there exists a unique Hilbert space  $\mathcal{H}_{\mathbb{K}}$  of functions  $h : \mathcal{X} \rightarrow \mathcal{Y}$  satisfying the two conditions:

- For all  $x \in \mathcal{X}$ ,  $\mathbb{K}(\cdot, x) \in \mathcal{L}(\mathcal{Y}, \mathcal{H}_{\mathbb{K}})$ .
- For all  $h \in \mathcal{H}_{\mathbb{K}}$ ,  $h(x) = \mathbb{K}(\cdot, x)^\# h$ .

Where  $\mathbb{K}(\cdot, x) \in \mathcal{L}(\mathcal{Y}, \mathcal{F}(\mathcal{X}, \mathcal{Y}))$  is an operator which associates to any  $y \in \mathcal{Y}$  the function  $\mathbb{K}(\cdot, x)y \in \mathcal{F}(\mathcal{X}, \mathcal{Y})$  defined by  $x' \mapsto \mathbb{K}(x', x)y \in \mathcal{Y}$ . The second condition is called the reproducing property, and it implies that for all  $x \in \mathcal{X}$ , for all  $y \in \mathcal{Y}$  and for all  $h \in \mathcal{H}_{\mathbb{K}}$ ,

$$\langle \mathbb{K}(\cdot, x)y, h \rangle_{\mathcal{H}_{\mathbb{K}}} = \langle y, h(x) \rangle_{\mathcal{Y}}. \quad (14)$$

The Hilbert space  $\mathcal{H}_{\mathbb{K}}$  is called the reproducing kernel Hilbert space associated to the kernel  $\mathbb{K}$ . This RKHS can be built by taking the closure of the set  $\{\mathbb{K}(\cdot, x)y \mid x \in \mathcal{X}, y \in \mathcal{Y}\}$ .

The scalar product on  $\mathcal{H}_{\mathbb{K}}$  between two functions  $h_0 = \sum_{i=1}^N \mathbb{K}(\cdot, x_i)y_i$  and  $h_1 = \sum_{j=1}^{N'} \mathbb{K}(\cdot, x'_j)y'_j$ ,  $x_i, x'_j \in \mathcal{X}$ ,  $y_i, y'_j \in \mathcal{Y}$ , is defined as:

$$\langle h_0, h_1 \rangle_{\mathcal{H}_{\mathbb{K}}} = \sum_{i=1}^N \sum_{j=1}^{N'} \langle y_i, \mathbb{K}(x_i, x'_j)y'_j \rangle_{\mathcal{Y}}.$$

The corresponding norm  $\|\cdot\|_{\mathcal{H}_{\mathbb{K}}}$  is defined by  $\|h\|_{\mathcal{H}_{\mathbb{K}}}^2 = \langle h, h \rangle_{\mathcal{H}_{\mathbb{K}}}$ .

Finally, we give the following Lemma which we use in the proofs. We now take  $\mathcal{Y} = \mathbb{R}^D$  which corresponds to the use of vv-RKHS we make in the core paper.



**Lemma A.1.** *Micchelli & Pontil (2005)* Let  $\mathcal{H}_K \subset \mathcal{F}(\mathcal{X}, \mathbb{R}^D)$  a vv-RKHS associated to a positive matrix-valued kernel  $K$ . Then we have for all  $x \in \mathcal{X}$ :

$$\|h(x)\|_{\mathbb{R}^D} \leq \|h\|_{\mathcal{H}_K} \|K(x, x)\|_{Op}^{1/2}.$$

## B Proofs for Section 3

### B.1 Proof of Proposition 3.1

We recall first the proposition which corresponds to Proposition 3.1 of the main paper. Given  $K : \mathcal{X} \times \mathcal{X} \mapsto \mathcal{L}(\mathbb{R}^D)$  an OVK with  $\mathcal{H}_K \subset \mathcal{F}(\mathcal{X}, \mathbb{R}^D)$  its associated vv-RKHS, we want to solve the following optimization problem

$$\min_{h \in \mathcal{H}_K} \frac{1}{N} \sum_{i=1}^N \ell(y_i, \Phi h(x_i)) + \lambda \|h\|_{\mathcal{H}_K}^2. \quad (15)$$

The Proposition

**Proposition B.1. (Representer theorem)** *If  $\ell$  is continuous and convex with respect to its second argument, the problem in Eq. (15) admits a unique minimizer  $\widehat{h}_{\mathcal{S}_N}$ . Moreover there exist  $(\alpha_j)_{j=1}^N \in \mathbb{R}^D$  such that  $\widehat{h}_{\mathcal{S}_N} = \sum_{j=1}^N K(\cdot, x_j) \alpha_j$ .*

**Proof of Proposition B.1 :** We denote the data-fitting term as:

$$J : h \mapsto \frac{1}{N} \sum_{i=1}^N \ell(y_i, \Phi h(x_i)) .$$

The loss is assumed to be continuous and convex with respect to the second argument. The objective  $h \mapsto J(h) + \frac{\lambda}{2} \|h\|_{\mathcal{H}_K}^2$  is thus a continuous and strictly convex function on  $\mathcal{H}_K$ —strictly because  $\lambda > 0$ .

As a consequence, it admits a unique minimizer on  $\mathcal{H}_K$  [Bauschke & Combettes \(2017\)](#), which we denote by  $\widehat{h}_{\mathcal{S}_N}$ .

Let  $\mathcal{U} := \left\{ h \mid h = \sum_{j=1}^N K(\cdot, x_j) \alpha_j, (\alpha_j)_{j=1}^N \in \mathbb{R}^D \right\}$ . Then  $\mathcal{U}$  is a closed subspace of  $\mathcal{H}_K$ , so we have the decomposition  $\mathcal{H}_K = \mathcal{U} \oplus \mathcal{U}^\perp$  and we can write  $\widehat{h}_{\mathcal{S}_N} = \widehat{h}_{\mathcal{U}} + \widehat{h}_{\mathcal{U}^\perp}$  with  $(\widehat{h}_{\mathcal{U}}, \widehat{h}_{\mathcal{U}^\perp}) \in \mathcal{U} \times \mathcal{U}^\perp$ . Now, for all  $i \in [N]$  and  $\theta \in \Theta$ , from [Theorem A.1](#), we have  $\langle \phi(\theta), \widehat{h}_{\mathcal{S}_N}(x_i) \rangle_{\mathbb{R}^D} = \langle K(\cdot, x_i) \phi(\theta), \widehat{h}_{\mathcal{S}_N} \rangle_{\mathcal{H}_K}$  and using that  $K(\cdot, x_i) \phi(\theta) \in \mathcal{U}$ , we get that

$$\langle \phi(\theta), \widehat{h}_{\mathcal{S}_N}(x_i) \rangle_{\mathbb{R}^D} = \langle K(\cdot, x_i) \phi(\theta), \widehat{h}_{\mathcal{U}} \rangle_{\mathcal{H}_K} = \langle \phi(\theta), \widehat{h}_{\mathcal{U}}(x_i) \rangle_{\mathbb{R}^D} .$$

Hence the loss part  $J_N$  in the criterion to minimize is unchanged when replacing  $\widehat{h}_{\mathcal{S}_N}$  by its projection  $\widehat{h}_{\mathcal{U}}$  onto  $\mathcal{U}$ . On the other hand the penalty  $\|\widehat{h}_{\mathcal{S}_N}\|_{\mathcal{H}_K}^2$  decreases if we replace  $\widehat{h}_{\mathcal{S}_N}$  by  $\widehat{h}_{\mathcal{U}}$ , hence we must have  $\widehat{h}_{\mathcal{S}_N} = \widehat{h}_{\mathcal{U}} \in \mathcal{U}$ .  $\square$

### B.2 Proof of Proposition 3.2

First, we recall the proposition which corresponds to Proposition 3.2 of the main paper. We want to solve the following problem corresponding to Eq. (10) of the main paper.

$$\min_{\alpha \in \mathbb{R}^{DN}} \frac{1}{N} \|\mathbf{y} - \Phi(N) \mathbf{K} \alpha\|_{L^2(\Theta)^N}^2 + \lambda \langle \alpha, \mathbf{K} \alpha \rangle_{\mathbb{R}^{ND}} . \quad (16)$$

**Proposition B.2. (Closed form solution)** *The minimum of the problem in Eq. (16) is achieved by any  $\alpha^*$  satisfying*

$$(\mathbf{K}(\Phi^\# \Phi)_{(N)} \mathbf{K} + N \lambda \mathbf{K}) \alpha^* := \mathbf{K} \Phi_{(N)}^\# \mathbf{y} , \quad (17)$$

which has at least one solution  $\alpha^* \in \mathbb{R}^{ND}$ . Moreover if  $\mathbf{K}$  is full rank then  $((\Phi^\# \Phi)_{(N)} \mathbf{K} + N \lambda \mathbf{I})$  is invertible and

$$\alpha^* := ((\Phi^\# \Phi)_{(N)} \mathbf{K} + N \lambda \mathbf{I})^{-1} \Phi_{(N)}^\# \mathbf{y} . \quad (18)$$

**Proof of Proposition B.2 :** Up to an additional term not depending on  $\alpha$ , the objective function in Pb. (10) of the paper is

$$\frac{1}{N} \|\Phi_{(N)} \mathbf{K} \alpha\|_{L^2(\Theta)^N}^2 - \frac{2}{N} \langle \mathbf{y}, \Phi_{(N)} \mathbf{K} \alpha \rangle_{L^2(\Theta)^N} + \lambda \langle \alpha, \mathbf{K} \alpha \rangle_{\mathbb{R}^{ND}} .$$

Using that  $(\Phi_{(N)})^\# \Phi_{(N)} = \Phi_{(N)}^\# \Phi_{(N)} = (\Phi^\# \Phi)_{(N)}$ , that  $\mathbf{K}^\# = \mathbf{K}$  and multiplying by  $N$ , this becomes

$$\begin{aligned} L(\alpha) &:= \langle \alpha, \mathbf{K}(\Phi^\# \Phi)_{(N)} \mathbf{K} \alpha \rangle_{\mathbb{R}^{ND}} - 2 \langle \Phi_{(N)}^\# \mathbf{y}, \mathbf{K} \alpha \rangle_{\mathbb{R}^{ND}} + N \lambda \langle \alpha, \mathbf{K} \alpha \rangle_{\mathbb{R}^{ND}} \\ &= \langle \alpha, \mathbf{K} ((\Phi^\# \Phi)_{(N)} \mathbf{K} + N \lambda \mathbf{I}) \alpha \rangle_{\mathbb{R}^{ND}} - 2 \langle \Phi_{(N)}^\# \mathbf{y}, \mathbf{K} \alpha \rangle_{\mathbb{R}^{ND}} . \end{aligned}$$

We recall that our aim is to prove the following, corresponding to Eq. (11) of the main paper

$$(\mathbf{K}(\Phi^\# \Phi)_{(N)} \mathbf{K} + N \lambda \mathbf{K}) \alpha^* = \mathbf{K} \Phi_{(N)}^\# \mathbf{y} . \quad (19)$$

Observe now that

$$\begin{aligned} \langle \alpha^*, \mathbf{K} ((\Phi^\# \Phi)_{(N)} \mathbf{K} + N \lambda \mathbf{I}) \alpha \rangle_{\mathbb{R}^{ND}} &= \langle \alpha, \mathbf{K} ((\Phi^\# \Phi)_{(N)} \mathbf{K} + N \lambda \mathbf{I}) \alpha^* \rangle_{\mathbb{R}^{ND}} \\ &= \langle \alpha, \mathbf{K} \Phi_{(N)}^\# \mathbf{y} \rangle_{\mathbb{R}^{ND}} \\ &= \langle \Phi_{(N)}^\# \mathbf{y}, \mathbf{K} \alpha \rangle_{\mathbb{R}^{ND}} . \end{aligned}$$

Using the last two displays, we deduce that

$$\begin{aligned} L(\alpha) &= \langle \alpha, \mathbf{K} ((\Phi^\# \Phi)_{(N)} \mathbf{K} + N \lambda \mathbf{I}) \alpha \rangle_{\mathbb{R}^{ND}} - 2 \langle \Phi_{(N)}^\# \mathbf{y}, \mathbf{K} \alpha \rangle_{\mathbb{R}^{ND}} \\ &= \langle \alpha - \alpha^*, \mathbf{K} ((\Phi^\# \Phi)_{(N)} \mathbf{K} + N \lambda \mathbf{I}) (\alpha - \alpha^*) \rangle_{\mathbb{R}^{ND}} \\ &\quad + \langle \alpha^*, \mathbf{K} ((\Phi^\# \Phi)_{(N)} \mathbf{K} + N \lambda \mathbf{I}) \alpha^* \rangle_{\mathbb{R}^{ND}} . \end{aligned}$$

Since  $\mathbf{K} ((\Phi^\# \Phi)_{(N)} \mathbf{K} + N \lambda \mathbf{I})$  is a non-negative symmetric matrix, we conclude that  $L(\alpha)$  is minimal at  $\alpha = \alpha^*$ .

We now show that (19) always has a solution  $\alpha^*$  in  $\mathbb{R}^{ND}$  and conclude with the special case where  $\mathbf{K}$  is full rank. Note that  $(\mathbf{K}(\Phi^\# \Phi)_{(N)} \mathbf{K} + N \lambda \mathbf{K})$  is a non-negative definite symmetric matrix and its null space is exactly that of  $\mathbf{K}$ . Hence it is bijective on the image of  $\mathbf{K}$ , which shows that (19) always has a solution. If  $\mathbf{K}$  is moreover full rank then

$$((\Phi^\# \Phi)_{(N)} \mathbf{K} + N \lambda \mathbf{I}) = \mathbf{K}^{-1} (\mathbf{K}(\Phi^\# \Phi)_{(N)} \mathbf{K} + N \lambda \mathbf{K})$$

is also invertible and we can simplify by  $\mathbf{K}$  on both sides of (19) and obtain the claimed formula for  $\alpha^*$ , which achieves the proof.  $\square$

### B.3 Proof of Proposition 3.3

Let us first recall here the main assumptions used hereafter.

**Assumption B.1.**  $\mathcal{Y}$  is bounded:  $\exists c_{\mathcal{Y}} \in \mathbb{R}, \forall y \in \mathcal{Y}, \|y\|_{L^2(\Theta, \mu)} \leq c_{\mathcal{Y}}$ .

**Assumption B.2.** The kernel is bounded in the sense of its operator norm:  $\exists c_{\mathcal{K}} \in \mathbb{R}, \forall x \in \mathcal{X}, \|\mathcal{K}(x, x)\|_{\mathcal{O}_p} \leq c_{\mathcal{K}}$ .

**Assumption B.3.** The dictionary  $\phi$  is a Riesz family in  $L^2(\Theta)$  with respectively lower and upper constants  $c_{\phi}$  and  $C_{\phi}$ .

These assumptions correspond respectively to Assumptions 3.1, 3.2 and 3.3 in the paper.

The proposition we want to prove corresponds to Proposition 3.3 of the main paper, we recall it here.

**Proposition B.3. (Bound on estimation error)** Suppose that Assumptions 3.1, 3.2 and 3.3 hold. Let  $\widehat{h}_{\mathcal{S}_N}^{(a)} := \arg \min_{h \in \mathcal{H}_{\mathcal{K}}(a)} \widehat{\mathcal{R}}(\Phi h, \mathcal{S}_N)$ . Then, we have for any  $\delta > 0$ , with probability  $1 - \delta$ :

$$\begin{aligned} & \mathcal{R}(\Phi \widehat{h}_{\mathcal{S}_N}^{(a)}) - \inf_{h \in \mathcal{H}_{\mathcal{K}}(a)} \mathcal{R}(\Phi h) \\ & \leq 8\sqrt{2}a C_{\phi} (c_{\mathcal{Y}}\sqrt{c_{\mathcal{K}}} + ac_{\mathcal{K}}C_{\phi}) \frac{\sqrt{D}}{\sqrt{N}} \\ & \quad + 6\sqrt{2}(c_{\mathcal{Y}}^2 + a^2C_{\phi}^2c_{\mathcal{K}} + 2ac_{\mathcal{Y}}C_{\phi}\sqrt{c_{\mathcal{K}}}) \sqrt{\frac{\log\left(\frac{4}{\delta}\right)}{N}}. \end{aligned}$$

For completeness, we restate the definition of the true risk and of the empirical risk.

**Definition B.1. (True risk)** Let  $g \in \mathcal{G} \subset \mathcal{F}(\mathcal{X}, L^2(\Theta))$  be an hypothesis class of functions and let  $(X, Y)$  be a couple of random variables on  $\mathcal{X} \times \mathcal{Y}$  with  $\mathcal{Y} \subset L^2(\Theta)$ . The true risk of  $g$  is given by

$$\mathcal{R}(g) := \mathbb{E}_{X, Y} [\ell(Y, g(X))].$$

**Definition B.2. (Empirical risk)** Let  $g \in \mathcal{G} \subset \mathcal{F}(\mathcal{X}, L^2(\Theta))$  be an hypothesis class of functions, let  $\mathcal{S}_N = (z_1, \dots, z_N)$  be a sample in  $\mathcal{Z} = \mathcal{X} \times L^2(\Theta)$  with for any  $i \in [N]$ ,  $z_i = (x_i, y_i)$ . For a given loss function  $\ell$  on  $L^2(\Theta)$ , the empirical risk of  $g$  on the sample  $\mathcal{S}_N$  is defined as

$$\widehat{\mathcal{R}}(g, \mathcal{S}_N) := \frac{1}{N} \sum_{i=1}^N \ell(y_i, g(x_i)).$$

We recall as well the following concentration inequality.

**Theorem B.1. (McDiarmid's inequality).** Let  $Z_1, \dots, Z_N$  be a set of independent random variables in  $\mathcal{Z}$ , assume that there exist  $a_1, \dots, a_N > 0$  such that  $f \in \mathcal{F}(\mathcal{Z}^N, \mathbb{R})$  satisfies for all  $i \in [N]$  and for all  $z_1, \dots, z_N, z'_i \in \mathcal{Z}$

$$|f(z_1, \dots, z_i, \dots, z_N) - f(z_1, \dots, z'_i, \dots, z_N)| \leq a_i.$$

Then for any  $\delta > 0$ , the following inequalities hold

$$\begin{aligned} \mathbb{P}[f(\mathcal{S}_N) - \mathbb{E}[f(\mathcal{S}_N)] \geq \delta] & \leq \exp\left(\frac{-2\delta^2}{\sum_{i=1}^N a_i^2}\right), \\ \mathbb{P}[f(\mathcal{S}_N) - \mathbb{E}[f(\mathcal{S}_N)] \leq -\delta] & \leq \exp\left(\frac{-2\delta^2}{\sum_{i=1}^N a_i^2}\right). \end{aligned}$$

We now restate the definition of the empirical Rademacher complexity and of the Rademacher complexity which we use extensively in the proof.

**Definition B.3. (Empirical Rademacher Complexity)** Let  $\mathcal{G} \subset \mathcal{F}(\mathcal{Z}, \mathbb{R})$  and let  $(z_1, \dots, z_N) \in \mathcal{Z}^N$  be a sample of size  $N$  with elements in a given set  $\mathcal{Z}$ . Let  $\sigma = (\sigma_i)_{i=1}^N$  be a sequence of i.i.d. Rademacher variables. The empirical Rademacher complexity of  $\mathcal{G}$  on the sample  $\mathcal{S}_N$  is defined as

$$\widehat{\mathfrak{R}}(\mathcal{G}, \mathcal{S}_N) := \mathbb{E}_{\sigma} \left[ \sup_{g \in \mathcal{G}} \frac{1}{N} \sum_{i=1}^N \sigma_i g(z_i) \right].$$

**Definition B.4. (Rademacher Complexity)** Let  $N \in \mathbb{N}$  and  $\mathcal{G} \subset \mathcal{F}(\mathcal{Z}, \mathbb{R})$ , the Rademacher complexity of  $\mathcal{G}$  on the samples of size  $N$  is defined as:

$$\mathfrak{R}_N(\mathcal{G}) := \mathbb{E}_{\mathcal{S}_N} \left[ \widehat{\mathfrak{R}}(\mathcal{G}, \mathcal{S}_N) \right].$$

We namely use the following lemma involving the Rademacher complexity in our proof.

**Lemma B.1.** *Let  $\mathcal{S}_N = (z_1, \dots, z_N) \subset \mathcal{Z}^N$  be an i.i.d. sample on  $\mathcal{Z}$ . Let  $\mathcal{G} \subset \mathcal{F}(\mathcal{Z}, \mathbb{R})$  and let  $\Psi(\mathcal{S}_N) := \sup_{g \in \mathcal{G}} (\mathcal{R}(g) - \widehat{\mathcal{R}}(g, \mathcal{S}_N))$ . Then, we have that*

$$\mathbb{E}_{\mathcal{S}_N}(\Psi(\mathcal{S}_N)) \leq 2\mathfrak{R}_N(\mathcal{G}).$$

*Proof.* This corresponds to the inequality (3.7) in the proof of Theorem 3.3 of [Mohri et al. \(2018\)](#).  $\square$

Finally, we introduce the following inequalities and lemmas.

Let  $(\phi_1, \dots, \phi_D)$  be a Riesz family (see Definition 2.1 of the main paper) and  $\Phi$  its associated projection operator (see Definition 2.2 of the main paper). Coupling the two definitions we have

$$c_{\phi} \|\gamma\|_{\mathbb{R}^D} \leq \|\Phi\gamma\|_{L^2(\Theta)} \leq C_{\phi} \|\gamma\|_{\mathbb{R}^D}. \quad (20)$$

Moreover, using the definition of the adjoint  $\Phi^{\#}$  of  $\Phi$  (Lemma 2.1 into the main paper) into Eq. (5) of the main paper yields for all  $f \in \text{Span}(\phi_1, \dots, \phi_D)$ ,

$$c_{\phi} \|f\|_{L^2(\Theta)} \leq \|\Phi^{\#}f\|_{\mathbb{R}^D} \leq C_{\phi} \|f\|_{L^2(\Theta)}. \quad (21)$$

**Lemma B.2.** *Under Assumptions B.2 and B.3, the set of function*

$\widetilde{\mathcal{Y}}_{K, \phi}(a) := \{\Phi h(x) : h \in \mathcal{H}_K(a), x \in \mathcal{X}\} \subset L_2(\Theta, \mu)$  *is bounded with respect to the  $\|\cdot\|_{L^2(\Theta)}$  norm with constant  $C_{\phi} \sqrt{c_K} a$ .*

*Proof.* We apply (20) with Lemma A.1, and then Assumption B.2.  $\square$

**Lemma B.3.** *Let  $\Psi(\mathcal{S}_N) := \sup_{h \in \mathcal{H}_K(a)} (\mathcal{R}(\Phi h) - \widehat{\mathcal{R}}(\Phi h, \mathcal{S}_N))$ . Under Assumptions B.1, B.2 and B.3, for any  $\delta > 0$ , we get with probability  $1 - \frac{\delta}{4}$  that*

$$\Psi(\mathcal{S}_N) \leq \mathbb{E}_{\mathcal{S}_N}(\Psi(\mathcal{S}_N)) + A \sqrt{\frac{\log(\frac{4}{\delta})}{2N}}.$$

*With the constant  $A$  defined as*

$$A := 2c_{\mathcal{Y}}^2 + 2C_{\phi}^2 a^2 c_K + 4c_{\mathcal{Y}} a C_{\phi} \sqrt{c_K}.$$

*Proof.* Let  $\mathcal{S}'_N$  be a sample differing from the sample  $\mathcal{S}_N$  by only one observation, for instance the last one which we set as  $(x_N, y_N)$  for  $\mathcal{S}_N$  and  $(x'_N, y'_N)$  for  $\mathcal{S}'_N$ .

We have that

$$\Psi(\mathcal{S}_N) - \Psi(\mathcal{S}'_N) \leq \sup_{h \in \mathcal{H}_K(a)} \left( \widehat{\mathcal{R}}(\Phi h, \mathcal{S}_N) - \widehat{\mathcal{R}}(\Phi h, \mathcal{S}'_N) \right).$$

Moreover,

$$\sup_{h \in \mathcal{H}_K(a)} \left( \widehat{\mathcal{R}}(\Phi h, \mathcal{S}_N) - \widehat{\mathcal{R}}(\Phi h, \mathcal{S}'_N) \right) = \sup_{h \in \mathcal{H}_K(a)} \left( \frac{\ell(y_N, \Phi h(x_N)) - \ell(y'_N, \Phi h(x'_N))}{N} \right). \quad (22)$$

Developing with the quadratic loss,

$$\frac{\ell(y_N, \Phi h(x_N)) - \ell(y'_N, \Phi h(x'_N))}{N} = \frac{\|y_N - \Phi h(x_N)\|_{\mathbb{L}^2(\Theta)}^2 - \|y'_N - \Phi h(x'_N)\|_{\mathbb{L}^2(\Theta)}^2}{N}.$$

Using Assumptions B.1, Assumption B.2 and Lemma B.2, we can then bound the numerator as

$$\begin{aligned} & \|y_N - \Phi h(x_N)\|_{\mathbb{L}^2(\Theta)}^2 - \|y'_N - \Phi h(x'_N)\|_{\mathbb{L}^2(\Theta)}^2 \\ & \leq \|y_N\|_{\mathbb{L}^2(\Theta)}^2 + \|y'_N\|_{\mathbb{L}^2(\Theta)}^2 + \|\Phi h(x_N)\|_{\mathbb{L}^2(\Theta)}^2 + \|\Phi h(x'_N)\|_{\mathbb{L}^2(\Theta)}^2 \\ & \quad + 2\langle y_N, \Phi h(x_N) \rangle_{L_2(\Theta, \mu)} + 2\langle y'_N, \Phi h(x'_N) \rangle_{L_2(\Theta, \mu)} \\ & \leq 2c_y^2 + 2C_\phi^2 a^2 c_K + 4c_y a C_\phi \sqrt{c_K}. \end{aligned}$$

We define a new constant  $A := 2c_y^2 + 2C_\phi^2 a^2 c_K + 4c_y a C_\phi \sqrt{c_K}$ .

Using McDiarmid's inequality (Theorem B.1), for any  $\delta > 0$ , we get with probability  $1 - \frac{\delta}{4}$  that

$$\Psi(\mathcal{S}_N) \leq \mathbb{E}_{\mathcal{S}_N}(\Psi(\mathcal{S}_N)) + A \sqrt{\frac{\log\left(\frac{4}{\delta}\right)}{2N}}.$$

□

**Lemma B.4.** *Under Assumptions B.1, B.2 and B.3, the Rademacher complexity of the family functions  $\ell \circ \mathcal{G}_{K, \phi}(a)$  defined in Eq. (40) can be bounded in terms of empirical Rademacher complexity with high probability. Namely, let  $\delta > 0$ , then with probability at least  $1 - \frac{\delta}{4}$ :*

$$\mathfrak{R}_N(\ell \circ \mathcal{G}_{K, \phi}(a)) \leq \widehat{\mathfrak{R}}(\ell \circ \mathcal{G}_{K, \phi}(a), \mathcal{S}_N) + A \sqrt{\frac{\log\left(\frac{4}{\delta}\right)}{2N}}. \quad (23)$$

*Proof.* Let  $\mathcal{S}_N$  and  $\mathcal{S}'_N$  be two samples in  $(\mathcal{X} \times \mathcal{Y})^N$  differing by only one observation, for instance the last one which is  $(x_N, y_N)$  for  $\mathcal{S}_N$  and  $(x'_N, y'_N)$  for  $\mathcal{S}'_N$ . We can bound the variation of the difference of the empirical Rademacher complexity on the two samples.

$$\begin{aligned}
 & \widehat{\mathfrak{R}}(\ell \circ \mathcal{G}_{\mathcal{K},\phi}(a), \mathcal{S}_N) - \widehat{\mathfrak{R}}(\ell \circ \mathcal{G}_{\mathcal{K},\phi}(a), \mathcal{S}'_N) \\
 &= \frac{1}{N} \mathbb{E}_{\sigma} \left[ \sup_{h \in \mathcal{H}_{\mathcal{K}}(a)} \left( \sum_{i=1}^N \sigma_i \ell(y_i, \Phi h(x_i)) \right) - \sup_{h \in \mathcal{H}_{\mathcal{K}}(a)} \left( \sum_{i=1}^{N-1} \sigma_i \ell(y_i, \Phi h(x_i)) + \sigma_N \ell(y'_N, \Phi h(x'_N)) \right) \right] \\
 &\leq \frac{1}{N} \mathbb{E}_{\sigma} \left[ \sup_{h \in \mathcal{H}_{\mathcal{K}}(a)} (\sigma_N (\ell(y_N, \Phi h(x_N)) - \ell(y'_N, \Phi h(x'_N)))) \right] \tag{24}
 \end{aligned}$$

$$\leq \sup_{h \in \mathcal{H}_{\mathcal{K}}(a)} \left( \frac{\ell(y_N, \Phi h(x_N)) - \ell(y'_N, \Phi h(x'_N))}{N} \right). \tag{25}$$

Where (24) stems from the fact that the difference of the suprema is smaller than the supremum of the difference, and (25) from the fact that Rademacher variables take their values in  $\{-1, 1\}$ .

We remark that this quantity is the same as the one we bound in the proof of Lemma B.3 in (22).

Thus we have

$$\widehat{\mathfrak{R}}(\ell \circ \mathcal{G}_{\mathcal{K},\phi}(a), \mathcal{S}_N) - \widehat{\mathfrak{R}}(\ell \circ \mathcal{G}_{\mathcal{K},\phi}(a), \mathcal{S}'_N) \leq \frac{A}{N}.$$

Then applying McDiarmid's inequality (Theorem B.1), for  $\delta > 0$ , we have with probability  $1 - \frac{\delta}{4}$ :

$$\mathfrak{R}_N(\ell \circ \mathcal{G}_{\mathcal{K},\phi}(a)) \leq \widehat{\mathfrak{R}}(\ell \circ \mathcal{G}_{\mathcal{K},\phi}(a), \mathcal{S}_N) + A \sqrt{\frac{\log(\frac{4}{\delta})}{2N}}.$$

□

**Lemma B.5.** *Suppose that Assumption B.1, B.2 and Assumption B.3 are verified and that  $\ell$  is the quadratic loss. Then for all  $a > 0$ , the empirical Rademacher complexity of the family of functions  $\ell \circ \mathcal{G}_{\mathcal{K},\phi}(a)$  defined in Eq. (40) satisfies*

$$\widehat{\mathfrak{R}}(\ell \circ \mathcal{G}_{\mathcal{K},\phi}(a), \mathcal{S}_N) \leq 2\sqrt{2} a C_{\phi} \sqrt{c_{\mathcal{K}}} (c_{\mathcal{Y}} + a C_{\phi} \sqrt{c_{\mathcal{K}}}) \frac{\sqrt{D}}{\sqrt{N}}. \tag{26}$$

*Proof.* Let  $e_1, \dots, e_D$  be an orthonormal basis of  $\text{Im}(\Phi)$ , which is a  $D$ -dimensional linear subspace of  $L_2(\Theta, \mu)$ . For the quadratic loss, for all  $i \in [N]$  and  $h \in \mathcal{H}_{\mathcal{K}}$ , we may write

$$\ell(y_i, \Phi h(x_i)) = \ell_i \left( \left( \langle \Phi h(x_i), e_k \rangle_{L_2(\Theta, \mu)} \right)_{k=1}^D \right),$$

where we set

$$\ell_i((u_k)_{k \in [D]}) = \sum_{k=1}^D (\langle y_i, e_k \rangle_{L_2(\Theta, \mu)} - u_k)^2.$$

We show that for any  $i \in [N]$ ,  $\ell_i$  is  $L$ -Lipschitz on the set  $\{u \in \mathbb{R}^D, \|u\|_{\mathbb{R}^D} \leq a \sqrt{C_{\phi} c_{\mathcal{K}}}\}$ , with  $L$  defined as

$$L := 2(c_{\mathcal{Y}} + a C_{\phi} \sqrt{c_{\mathcal{K}}}). \tag{27}$$

We define for all  $i \in [N]$  and for all  $k \in [D]$ ,  $y_{ik} := \langle y_i, e_k \rangle_{L_2(\Theta, \mu)}$ .

Let  $u, v \in \mathbb{R}^D$  such that  $\|u\|_{\mathbb{R}^D} \leq aC_\phi\sqrt{c_K}$  and  $\|v\|_{\mathbb{R}^D} \leq aC_\phi\sqrt{c_K}$ , then for all  $i \in [N]$

$$\left| \sum_{k=1}^D (y_{ik} - u_k)^2 - \sum_{k=1}^D (y_{ik} - v_k)^2 \right| \leq \sum_{k=1}^D |u_k - v_k| |2y_{ik} - (u_k + v_k)| \quad (28)$$

$$\leq \|u - v\|_{\mathbb{R}^D} \sqrt{\sum_{k=1}^D (2y_{ik} - u_k - v_k)^2} \quad (29)$$

$$\leq \|u - v\|_{\mathbb{R}^D} (2\|(y_{ik})_{k \in [D]}\|_{\mathbb{R}^D} + \|u\|_{\mathbb{R}^D} + \|v\|_{\mathbb{R}^D}) \quad (30)$$

$$\leq 2(c_Y + aC_\phi\sqrt{c_K}) \|u - v\|_{\mathbb{R}^D}. \quad (31)$$

Where (28) stems from factorizing and using Minkowski's inequality, (29) comes from applying Cauchy-Schwartz, (30) comes from applying Minkowski's inequality and (31) is a consequence of the fact that  $\|(y_{ik})_{k \in [D]}\|_{\mathbb{R}^D} \leq \|y_i\|_{L^2(\Theta)}$  combined with Assumption B.1 as well as the assumptions on  $u$  and  $v$ .

We highlight that for all  $i \in [N]$ , using Lemma B.2 and the orthonormality of  $e_1, \dots, e_D$ ,  $\|(\langle \Phi h(x_i), e_k \rangle_{L^2(\Theta)})_{k \in [D]}\|_{\mathbb{R}^D} = \|\Phi h(x_i)\|_{L^2(\Theta)} \leq aC_\phi\sqrt{c_K}$ .

As a consequence, we can use Corollary 1 from Maurer (2016) to obtain

$$\widehat{\mathfrak{R}}(\ell \circ \mathcal{G}_{K,\phi}(a), \mathcal{S}_N) \leq \frac{\sqrt{2}L}{N} \mathbb{E} \left[ \sup_{h \in \mathcal{H}_K(a)} \left( \sum_{i=1}^N \sum_{k=1}^D \sigma_{ik} \langle \Phi h(x_i), e_k \rangle_{L^2(\Theta, \mu)} \right) \right]. \quad (32)$$

We now rewrite the expectation in the right-hand side as

$$\begin{aligned} \mathbb{E} \left[ \sup_{h \in \mathcal{H}_K(a)} \left( \sum_{i=1}^N \sum_{k=1}^D \sigma_{ik} \langle \Phi h(x_i), e_k \rangle_{L^2(\Theta, \mu)} \right) \right] &= \mathbb{E} \left[ \sup_{h \in \mathcal{H}_K(a)} \left( \sum_{i=1}^N \sum_{k=1}^D \sigma_{ik} \langle h(x_i), \Phi^\# e_k \rangle_{\mathbb{R}^D} \right) \right] \\ &= \mathbb{E} \left[ \sup_{h \in \mathcal{H}_K(a)} \left( \sum_{i=1}^N \sum_{k=1}^D \sigma_{ik} \langle h, \mathcal{K}(\cdot, x_i) \Phi^\# e_k \rangle_{\mathcal{H}_K} \right) \right] \\ &= \mathbb{E} \left[ \sup_{h \in \mathcal{H}_K(a)} \left( \left\langle h, \sum_{i=1}^N \sum_{k=1}^D \sigma_{ik} \mathcal{K}(\cdot, x_i) \Phi^\# e_k \right\rangle_{\mathcal{H}_K} \right) \right]. \end{aligned} \quad (33)$$

Where (33) comes the reproducing property (Theorem A.1).

We now bound the obtained quantity in several steps. First, applying Cauchy-Schwartz yields

$$\mathbb{E} \left[ \sup_{h \in \mathcal{H}_K(a)} \left( \left\langle h, \sum_{i=1}^N \sum_{k=1}^D \sigma_{ik} \mathcal{K}(\cdot, x_i) \Phi^\# e_k \right\rangle_{\mathcal{H}_K} \right) \right] \leq a \mathbb{E} \left[ \left\| \sum_{i=1}^N \sum_{k=1}^D \sigma_{ik} \mathcal{K}(\cdot, x_i) \Phi^\# e_k \right\|_{\mathcal{H}_K} \right] \quad (35)$$

$$\leq a \sqrt{\mathbb{E} \left[ \left\| \sum_{i=1}^N \sum_{k=1}^D \sigma_{ik} \mathcal{K}(\cdot, x_i) \Phi^\# e_k \right\|_{\mathcal{H}_K}^2 \right]}. \quad (36)$$

Where we have applied Jensen's inequality to the square root function to obtain (36). Since  $(\sigma_{ik})_{i=1,k=1}^{N,D}$  is a centered i.i.d. sequence with values in the set  $\{-1, 1\}$ , we have

$$\begin{aligned} \mathbb{E} \left[ \left\| \sum_{i=1}^N \sum_{k=1}^D \sigma_{ik} \mathbf{K}(\cdot, x_i) \Phi^\# e_k \right\|_{\mathcal{H}_K}^2 \right] &= \sum_{i=1}^N \sum_{k=1}^D \left\| \mathbf{K}(\cdot, x_i) \Phi^\# e_k \right\|_{\mathcal{H}_K}^2 \\ &= \sum_{i=1}^N \sum_{k=1}^D \langle \Phi^\# e_k, \mathbf{K}(x_i, x_i) \Phi^\# e_k \rangle_{\mathbb{R}^D} . \end{aligned} \quad (37)$$

Where we have used the reproducing property (Theorem A.1) for (37).

Using the Cauchy-Schwartz inequality with Assumption B.2 and then (21)—which follows from Assumption B.3—combined with the fact that  $(e_k)_{k=1}^D$  is a normed family, we get that

$$\sum_{i=1}^N \sum_{k=1}^D \langle \Phi^\# e_k, \mathbf{K}(x_i, x_i) \Phi^\# e_k \rangle_{\mathbb{R}^D} \leq c_K \sum_{i=1}^N \sum_{k=1}^D \left\| \Phi^\# e_k \right\|_{\mathbb{R}^D}^2 \leq DN c_K C_\phi^2 . \quad (38)$$

Using (38) into (37), we combine the obtained result with (36) to obtain a majorant of the left-hand side of (34). Combining the resulting inequality with (32) and using the definition of  $L$  in (27) concludes the proof.  $\square$

**Proof of Proposition 3.3 :** A classic argument in statistical learning establishes the inequality

$$\mathcal{R}(\widehat{\Phi h}_{\mathcal{S}_N}) - \inf_{h \in \mathcal{H}_K(a)} \mathcal{R}(\Phi h) \leq 2 \sup_{h \in \mathcal{H}_K(a)} |\mathcal{R}(\Phi h) - \widehat{\mathcal{R}}(\Phi h, \mathcal{S}_N)| . \quad (39)$$

The first step of the proof consists in bounding the right side of the inequality in terms of Rademacher complexity.

To do so, we define the family of functions  $\mathcal{G}_{K,\phi}(a)$  by

$$\ell \circ \mathcal{G}_{K,\phi}(a) := \{x, y \mapsto \ell(y, \Phi h(x)), \quad h \in \mathcal{H}_K(a)\} . \quad (40)$$

We define as well  $\Psi(\mathcal{S}_N) := \sup_{h \in \mathcal{H}_K(a)} (\mathcal{R}(\Phi h) - \widehat{\mathcal{R}}(\Phi h, \mathcal{S}_N))$  which corresponds to the right term of (39) without the absolute value and without the coefficient 2. We then bound this term in terms of Rademacher complexity.

Lemma B.3 gives us that for  $\delta > 0$  with probability  $1 - \frac{\delta}{4}$ :

$$\Psi(\mathcal{S}_N) \leq \mathbb{E}_{\mathcal{S}_N}(\Psi(\mathcal{S}_N)) + A \sqrt{\frac{\log(\frac{2}{\delta})}{2N}} . \quad (41)$$

Applying Lemma B.1 yields

$$\mathbb{E}_{\mathcal{S}_N}(\Psi(\mathcal{S}_N)) \leq 2\mathfrak{N}_N(\ell \circ \mathcal{G}_{K,\phi}(a)) . \quad (42)$$

As a consequence combining this with (41) implies that still with probability  $1 - \frac{\delta}{4}$ :

$$\Psi(\mathcal{S}_N) \leq 2\mathfrak{N}_N(\ell \circ \mathcal{G}_{K,\phi}(a)) + A \sqrt{\frac{\log(\frac{4}{\delta})}{2N}} \quad (43)$$



We next bound the Rademacher complexity in terms of empirical Rademacher complexity. Using Lemma B.4, for  $\delta > 0$ , we have with probability  $1 - \frac{\delta}{4}$ :

$$\mathfrak{R}_N(\ell \circ \mathcal{G}_{\mathcal{K},\phi}(a)) \leq \widehat{\mathfrak{R}}(\ell \circ \mathcal{G}_{\mathcal{K},\phi}(a), \mathcal{S}_N) + A \sqrt{\frac{\log(\frac{4}{\delta})}{2N}}. \quad (44)$$

Using the union bound, combining (43) with (44) we get with probability  $1 - \frac{\delta}{2}$ :

$$\sup_{h \in \mathcal{H}_{\mathcal{K}}(a)} (\mathcal{R}(\Phi h) - \widehat{\mathcal{R}}(\Phi h, \mathcal{S}_N)) \leq 2\widehat{\mathfrak{R}}(\ell \circ \mathcal{G}_{\mathcal{K},\phi}(a), \mathcal{S}_N) + 3A \sqrt{\frac{\log(\frac{4}{\delta})}{2N}}. \quad (45)$$

Note that there is no  $|\cdot|$  on the left-hand side. The other hand is obtained by a symmetric argument.

Combining the obtained full inequality with (39) yields for any  $\delta > 0$ , with probability  $1 - \delta$ :

$$\mathcal{R}(\widehat{\Phi h}_{\mathcal{S}_N}) - \inf_{h \in \mathcal{H}_{\mathcal{K}}(a)} \mathcal{R}(\Phi h) \leq 4\widehat{\mathfrak{R}}(\ell \circ \mathcal{G}_{\mathcal{K},\phi}(a), \mathcal{S}_N) + 6A \sqrt{\frac{\log(\frac{4}{\delta})}{2N}}. \quad (46)$$

Then, using Lemma B.5 to bound the empirical Rademacher complexity concludes the proof.  $\square$

## C Supplements on the experiments

To avoid mentioning it repeatedly, we highlight now that when performing cross-validation, we use 5 folds in all the experiments.

### C.1 Toy dataset

#### C.1.1 Generating process

We consider first a functional toy dataset. To generate an instance we draw a set of  $P \in \mathbb{N}^*$  frequencies  $\omega \in (\mathbb{N}^*)^P$  uniformly at random without replacement in the set  $[\omega_{\max}]$  with  $\omega_{\max} \in \mathbb{N}^*$ . We then draw  $P$  coefficients  $a \in \mathbb{R}^P$  i.i.d according to a uniform distribution  $\mathcal{U}([-c_{\max}, c_{\max}])$ . Let  $w \in \mathbb{R}_+^*$  be a given width parameter. For  $p \in [P]$ , let  $B_4$  denote a cubic B-spline with knots set at the locations  $(-\frac{w}{2}, -\frac{w}{4}, 0, \frac{w}{4}, \frac{w}{2})$ —thus for instance for  $w = 3$  this corresponds to a classic cardinal B-spline de Boor (2001) except that it is centered at 0. From there, we define an input function  $x(t) := \sum_{p=1}^P a_p \cos(\omega_p t)$  with  $t \in \text{dom}_x := [0, 2\pi]$  and its corresponding output function  $y(t) := \sum_{p=1}^P a_p B_4(\omega_p - t)$  with  $t \in \text{dom}_y := [1 - \frac{w}{2}, \omega_{\max} + \frac{w}{2}]$ . In practice, we observe  $x$  and  $y$  on regular grids in their domains with respectively  $m_x \in \mathbb{N}^*$  and  $m_y \in \mathbb{N}^*$  discretization points. The experiments on this dataset are performed with  $P = 4$ ,  $\omega_{\max} = 10$ ,  $c_{\max} = 1$ ,  $w = 2$ ,  $m_x = 200$ ,  $m_y = 200$ . However for the experiments with missing data,  $m_y$  varies in which case we explicitly say so. Finally we add a centered Gaussian noise on the input observations with standard deviation  $\sigma_x = 0.07$  in all experiments. Examples of data generated that way with a Gaussian noise with standard deviation  $\sigma_y = 0.02$  added on the output observations are shown in Figure 3.

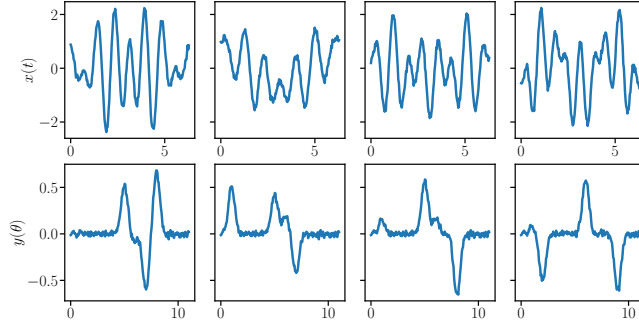


Figure 3: Examples of generated toy data, first row are the input functions and second row are their corresponding output functions.

### C.1.2 Experimental process and tuning

In all the experiments in this subsection, we use the dictionary perfectly adapted to the problem  $\phi := \{t \mapsto B_4(\omega - t), \omega \in [\omega_{\max}]\}$  and the separable kernel  $\mathbb{K}(x_0, x_1) := k(x_0, x_1)$  with  $k$  a scalar-valued Gaussian kernel with standard deviation  $\gamma = 20$ . We consider a training set of  $N_{\text{train}} = 500$  train samples and a testing set  $N_{\text{test}} = 300$  test samples.

**Robustness to noise.** In this first experiment, we focus on the effect of a first type of corruption of the output functions. We consider 50 Gaussian noise levels characterized by their standard deviations ranging from  $\sigma_y = 0$  to  $\sigma_y = 1.5$ . For each level of noise, regularization must be able to increase with the noise level. As a consequence, we cross-validate the regularization parameter  $\lambda$  for each level on a geometric grid of size 100 ranging from  $10^{-8}$  to  $10^{-3}$ . We then fit the regressor on the full train set with the selected  $\lambda$  and report the score on the test set. We in turn use this score to compute the signal to noise ratio defined as  $\text{SNR} := \frac{\frac{1}{N} \sum_{i=1}^N \frac{1}{M_i} \sum_{m=1}^{M_i} |y_{tm}^{\text{obs}}|}{\sigma_y}$ . The results are presented in Figure 1 of the main paper.

**Robustness to missing data.** For this second experiment we essentially use the same setting. However, the output noise level is now fixed at  $\sigma_y = 0.02$  and we remove uniformly at random a given percentage of the evaluations for each training output function. We do so to several extents, ranging from 0 % to 90 % of evaluations missing. These experiments are performed for several number of training samples size as well ( $N_{\text{train}} = 20, 50, 100, 250, 500$ ). For each configuration we allow the regularization parameter to change selecting it by cross-validation as in the previous experiment. The results are presented in Figure 2 of the main paper.

## C.2 DTI dataset

### C.2.1 More extensive description of the dataset

We now consider a Diffusion Tensor Imaging dataset <sup>1</sup>. This dataset was collected at Johns Hopkins University and the Kennedy-Krieger Institute. It consists of two Fractional anisotropy (FA) profiles inferred from the DTI scans. They are given along two tracts—the corpus callosum (CCA) one and the right corticospinal (RCS) one. It contains 382 such profiles from 142 subjects, 100 subjects suffering from multiple sclerosis (MS) and 42 healthy controls.

<sup>1</sup>This dataset is freely available as a part of the *Refund* R package

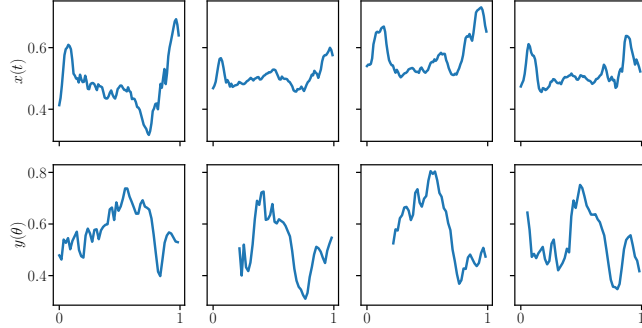


Figure 4: Examples of observations from the DTI dataset, first row are the input functions and second row are their corresponding output functions.

MS is an auto-immune disease which causes the immune system to gradually destroy myelin—the substance that isolates and protects the axons of nerve cells—, resulting in brain lesions and severe disability. FA profiles are frequently used as an indicator for demyelification as it causes a degradation of the diffusivity of the nerve tissues. The latter process is however not well understood and does not occur uniformly in the regions of the brain. We thus propose here to use our method to try to predict FA profiles along the RCS from FA profiles along the CCA. So as to remain in an i.i.d framework, we consider only the first scans of MS patients resulting in  $N = 100$  pairs of functions. The functions are observed at  $m_x = 93$  locations for the CCA tract and at  $m_y = 54$  locations for the RCS tract, however especially for the output functions, some chunks are missing at the beginning, we are thus dealing with sparsely observed functional data. Examples of instances from this dataset are shown in Figure 4.

### C.2.2 Experimental setting and tuning process

Since very few values are missing for the input functions, we use linear interpolation yielding regularly observed input functions. However, the number of missing values for the output functions is much more significant, so we do not perform such interpolation if it is not necessary—for 3BE, KPL and KE. However, the two other methods—KAM and FKRR—need densely observed functions, so we perform smoothing using linear interpolation as a first fitting step. For all the methods except KE, we center the output data upon training and added back the corresponding mean function to the predictions. We use  $N_{\text{train}} = 70$  data points for training and  $N_{\text{test}} = 30$  data points for testing. Finally, when we use dictionaries of wavelets, we extend the signal symmetrically to avoid affecting the coefficients on the boundaries of the interval of interest. We now give the full details of the the tuning process for each method.

- **KE.** We use a Gaussian kernel and cross-validate its variance parameter in a grid ranging from 0.02 to 1 with 100 points.
- **KPL.** We select the dictionary by cross-validation among different wavelets families. More precisely, we consider dictionaries of Daubechies wavelets and Coiflets wavelets [Daubechies & Heil \(1992\)](#) both with 2 and 3 vanishing moments and 4 and 5 dilatation levels. We cross-validate at the same time the regularization parameter  $\lambda$  on a geometric grid of size 100 ranging from  $10^{-9}$  to 1. We use a separable kernel of the form  $K(x_0, x_1) = k(x_0, x_1)D$

with  $k$  a Gaussian kernel with fixed standard deviation parameter  $\gamma = 0.9$ . The matrix  $D$  is a diagonal matrix of weights decreasing geometrically with the scale of the wavelet at the rate  $\frac{1}{b}$ —meaning for instance that at the  $j$ -th scale, the corresponding coefficients in the matrix are set to  $\frac{1}{b^j}$ . We cross-validate this parameter  $b$  as well considering values  $b \in \{1, 1.2, 1.4, 1.6\}$ .

- **3BE.** We tried several combinations for the input dictionary, however we did not cross-validate all those combinations together. We tried wavelets for both inputs and outputs (with the same configurations as for **KPL**), as well a mixed strategy with a Fourier basis for the inputs and a wavelet basis for the outputs. Finally, we tried Fourier bases for both the inputs and the outputs. Surprisingly, that latter configuration yielded better results. As a consequence, it is the one we use for the full experiment. We then cross-validate the highest frequency of the input basis  $\omega_{\text{in}}$ , that of the output basis  $\omega_{\text{out}}$ , the regularization parameter  $\lambda$  and the standard deviation parameter  $\gamma$  of the approximated Gaussian kernel. We use 300 Random Fourier Features for this approximation [Rahimi & Recht \(2008\)](#). More precisely, we consider the following grids:

- $\omega_{\text{in}} \in \{5, 10, 15, 20, 25, 30, 35, 40\}$
- $\omega_{\text{out}} \in \{5, 10, 15, 20, 25, 30, 35, 40\}$
- $\gamma \in \{20, 25, 30, 35, 40\}$
- $\lambda$  in a geometric grid of size 100 ranging from  $10^{-9}$  to 1.

- **KAM.** As highlighted in Section 4, the kernel in this method is a bit particular. It is defined on the following domain  $\kappa : ([0, 1] \times [0, 1] \times \mathbb{R})^2 \rightarrow \mathbb{R}$ . The first domain in the product corresponds to the domain of the input functions, the second to that of the output functions and the third one to the range of values of the input functions. In practice, as the authors [Reimherr & Sriperumbudur \(2017\)](#), we decouple the effect of the three variables in a product of three kernels which simplifies greatly the computations. We consider the following product of Gaussian kernels  $\kappa : ((s, t, v), (s', t', v')) \mapsto \exp\left(\frac{-(s-s')^2}{\gamma_1^2}\right) \exp\left(\frac{-(t-t')^2}{\gamma_2^2}\right) \exp\left(\frac{-(v-v')^2}{\gamma_3^2}\right)$ . We cross-validate together those three bandwidth parameters, the regularization parameter  $\lambda$  and the number of principal functions  $J$  used in the approximation considering the following values:

- $\gamma_1 \in \{0.01, 0.025, 0.05, 0.1\}$
- $\gamma_2 \in \{0.01, 0.025, 0.05, 0.1\}$
- $\gamma_3 \in \{0.03, 0.06, 0.1\}$
- $J \in \{10, 15, 20, 30\}$ .
- $\lambda$  in a geometric grid of size 100 ranging from  $10^{-9}$  to 1.

- **FKRR.** We use as kernel  $K(x_0, x_1) = k(x_0, x_1)\mathbb{T}$  with  $k$  a scalar Gaussian kernel and  $\mathbb{T} \in \mathcal{L}(\mathbb{L}^2(\Theta), \mathbb{L}^2(\Theta))$  defined as  $\mathbb{T}y(\theta_0) \mapsto \int_{\theta \in \Theta} \exp(-\beta|\theta_0 - \theta|)d\theta$ . In practice, we approximate the problem on an evenly spaced grid of size 200 and fix the standard deviation of the input Gaussian kernel to  $\gamma = 0.9$ . We select by cross-validation the parameter  $\beta$  of the output kernel and the regularization parameter  $\lambda$ . We use cross-validation as well to determine whether to center the data. We consider the following values for the parameters

- $\beta \in \{0.01, 0.025, 0.05, 0.75, 0.1, 0.125, 0.15, 0.2, 0.25, 0.3, 0.4, 0.5, 0.75, 1\}$
- $\lambda$  in a geometric grid ranging from  $10^{-7}$  to  $10^{-2}$  of size 100.

### C.3 Speech dataset

#### C.3.1 Description of the dataset

This object of this dataset is to study the speech inversion problem. From a given acoustic speech signal, the aim is to estimate the underlying vocal tract configuration that produced it [Richmond \(2002\)](#). It is motivated by several applications, for instance articulatory information can be used to improve the performance of speech recognition systems or to improve the speech synthesis quality in artificial voices. The dataset was introduced by [Mitra et al. \(2009\)](#) and proposed as a benchmark in [Kadri et al. \(2016\)](#). It is generated by a software which synthesizes words from an articulatory model and consists of a corpus of  $N = 413$  audio files of pronounced words along with the monitoring of the vocal tracts used to produce the corresponding sound. There are 8 of them: lip aperture (LA), lip protrusion (LP), tongue tip constriction degree (TTCD), tongue tip constriction location (TTCL), tongue body constriction degree (TBCD), tongue body constriction location (TBCL), Velum (VEL) and Glottis (GLO).

#### C.3.2 Experimental setting and tuning process

Since the duration of the words vary greatly, we pad both the input sounds and the 8 output vocal tracts by repeating the signals symmetrically to avoid continuity issue. Doing so we get inputs and outputs of the length of the longest word in the dataset. We represent the input sounds using 13 mel cepstral coefficients (MFCCs) acquired each 5ms with a window duration of 10ms. We use  $N_{\text{train}} = 300$  instances for training and  $N_{\text{test}} = 113$  for testing. Finally, we normalize the domain of the output functions to be  $[0, 1]$  as well as the range of values of the functions themselves to be  $[-1, 1]$  in order to have scores of the same magnitude for the different vocal tracts.

**Overview of the tuning performed on the methods.** We use the same input kernel for all the methods. It consists of a sum of 13 Gaussian kernels using the following normalization. Let  $(x_i^{(l)})_{i=1}^{N_{\text{train}}}$  be the vectors corresponding to the  $l$ -th MFCC with  $l \in [13]$ , the  $l$ -th kernel in the sum of kernels is

$$u, v \mapsto \exp\left(\frac{-\|u - v\|^2}{\gamma^2 \sum_{i=1}^{N_{\text{train}}} \|x_i^{(l)}\|^2}\right).$$

In practice, we set for all the methods  $\gamma = 1$  except for KE. We then perform the following individual tuning for the different methods, using the same tuning process for all the 8 vocal tract variables.

- **KE.** We cross-validated the parameter  $\gamma$  considering a grid ranging from 0.1 to 2 with a precision of 0.1.
- **KPL.** We use this time a data-dependant dictionary obtained by computing the functional principal components [Ramsay & Silverman \(2005\)](#) of the output functions on the training data. We keep only the one associated with the  $J$  largest eigenvalues. Using 5 folds, we cross-validated the regularization parameter  $\lambda$  along with  $J$ . We considered a geometric grid between  $10^{-11}$  and  $10^{-5}$  of size 50 for  $\lambda$  and  $J \in \{20, 30, 40\}$ .
- **3BE.** We use the same output basis as for KPL and the same tuning process as well. Note that since the MFCCs cannot be represented as smooth functions, we regress directly those MFCCs on the output coordinates on the principal functions. Thus, we do so using kernel ridge regressions rather than the approximated Kernel Ridge with Random Fourier Features used by the authors [Oliva et al. \(2015\)](#).

- **FKRR.** We use as output operator  $\mathbb{T} \in \mathcal{L}(\mathcal{L}^2(\Theta), \mathcal{L}^2(\Theta))$  defined as  $\mathbb{T}y(\theta_0) \mapsto \int_{\theta \in \Theta} \exp(-\beta|\theta_0 - \theta|)d\theta$ . We approximate in practice the problem on a evenly spaced grid of size 300. We cross-validate the parameter  $\beta$  of the output kernel along with the regularization parameter  $\lambda$  considering the following grids:
  - $\beta \in \{0.02, 0.03, 0.04, 0.05, 0.06, 0.07, 0.08, 0.09, 0.1, 0.125, 0.15\}$
  - $\lambda$  in a geometric grid of size 40 ranging from  $10^{-11}$  to  $10^{-5}$ .